Electronic Supporting Information for

Strong Two-photon Absorption and Ultrafast Dynamics in *Meso*-Functionalized "Push-Pull" *Trans*-A_2BC Porphyrins

Sandeep Kumar,[a] Jitendra Nath Acharyya,[b] Dipanjan Banerjee,[c] Venugopal Rao Soma,[c,*] G. Vijaya Prakash[b,*] and Muniappan Sankar[a,*]

[a]Department of Chemistry, Indian Institute of Technology Roorkee, Roorkee 247667, India.

[b]Nanophotonics Lab, Department of Physics, Indian Institute of Technology Delhi, Hauz Khas, New Delhi 110016, India

[c]Advanced Centre of Research in High Energy Materials (ACRHEM), University of Hyderabad, Hyderabad 500046, Telangana, India

*Authors for Correspondence: soma_venu@uohyd.ac.in; prakash@physics.iitd.ac.in; m.sankar@cy.iitr.ac.in

Table of Contents:

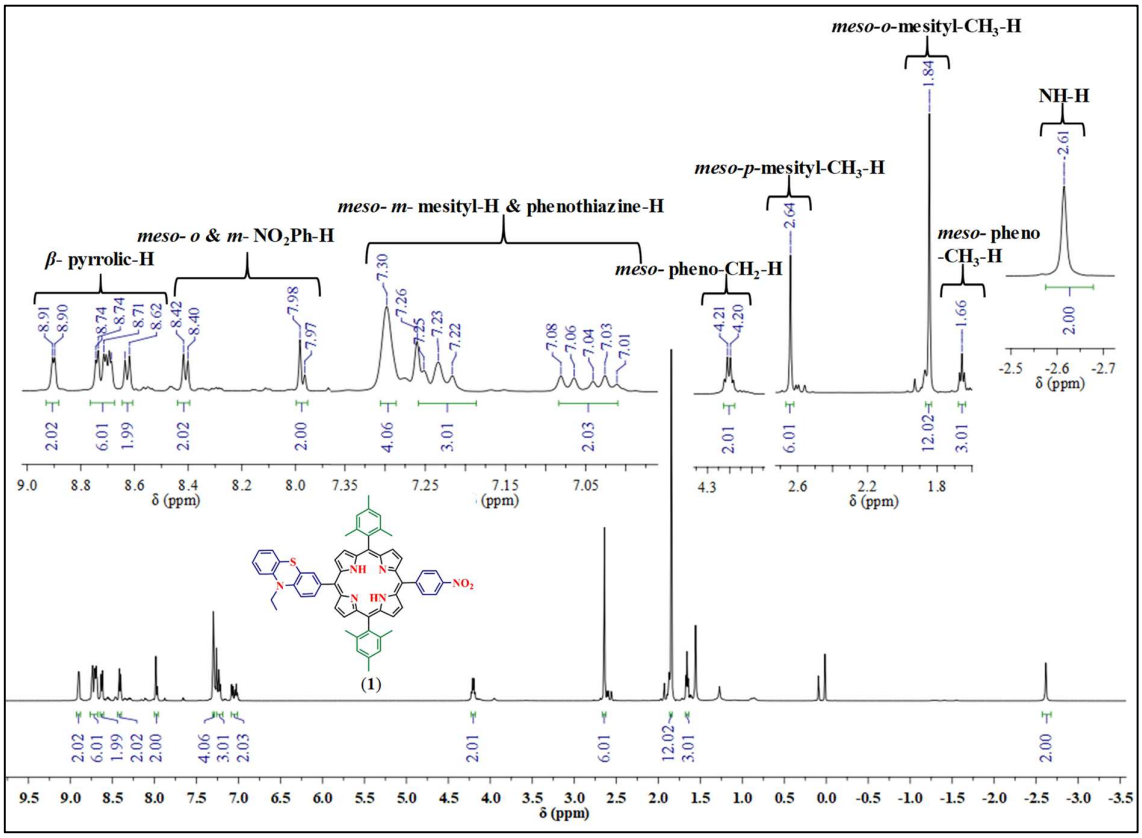

Figure S1 ^{1}H NMR of *trans*-H_2A_2BC (**1**) in $CDCl_3$ at 298 K.

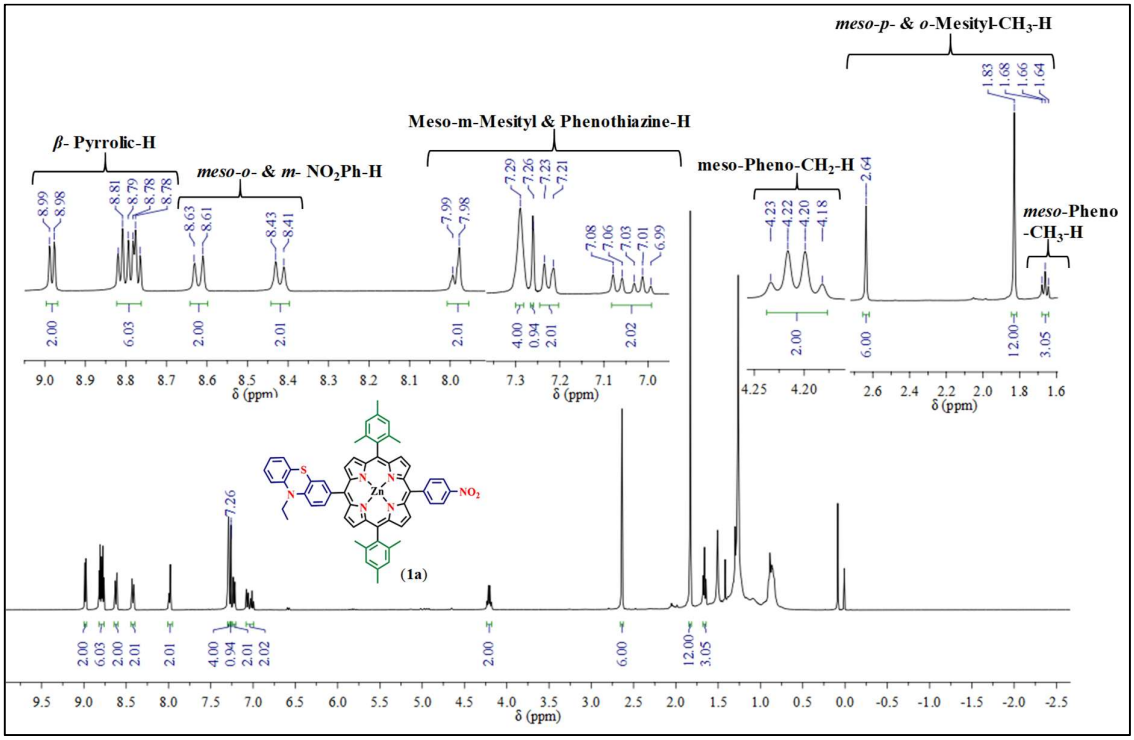

Figure S2 ^{1}H NMR of *trans*-ZnA_2BC (**1a**) in $CDCl_3$ at 298 K.

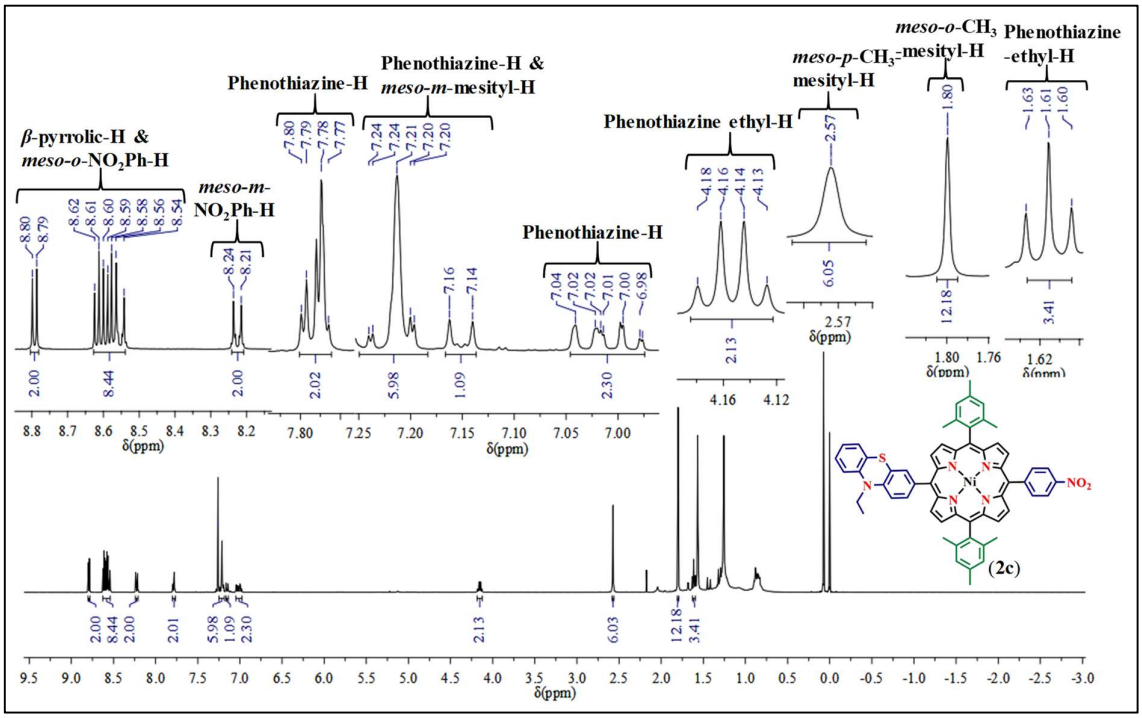

Figure S3 ^{1}H NMR of *trans*-NiA$_2$BC (**1c**) in CDCl$_3$ at 298 K.

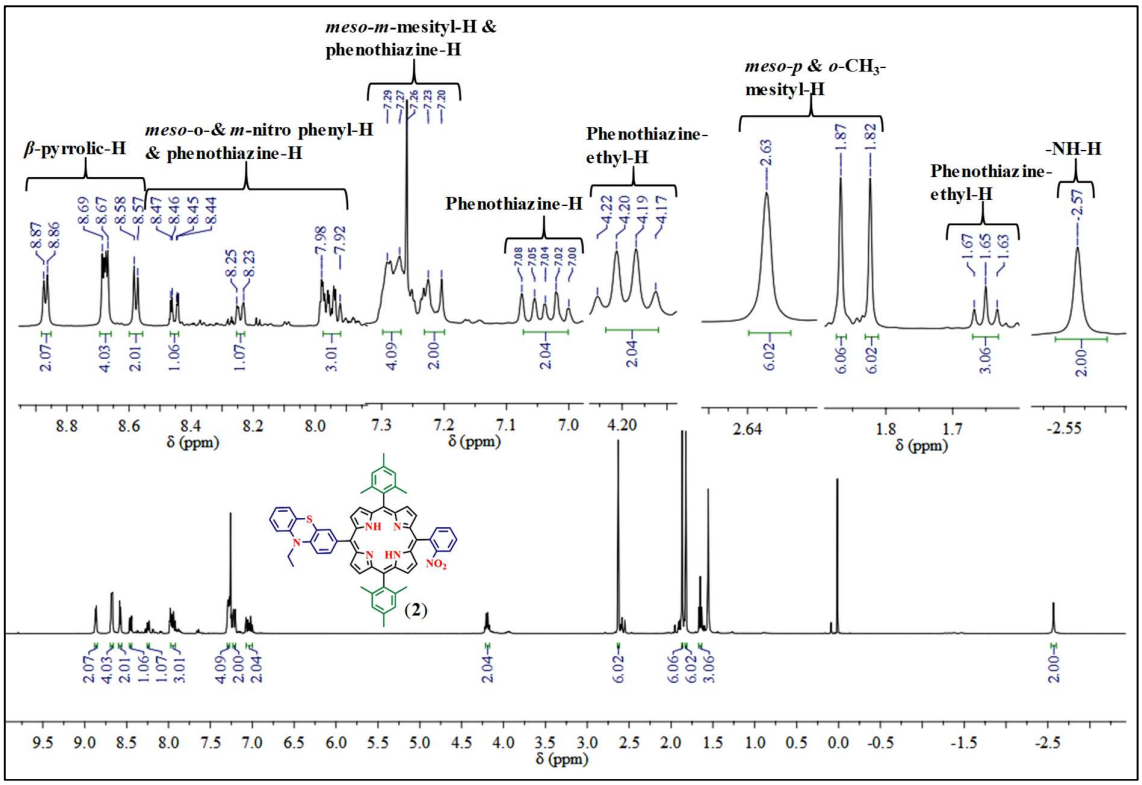

Figure S4 ^{1}H NMR of *trans*-H$_2$A$_2$BC (**2**) in CDCl$_3$ at 298 K.

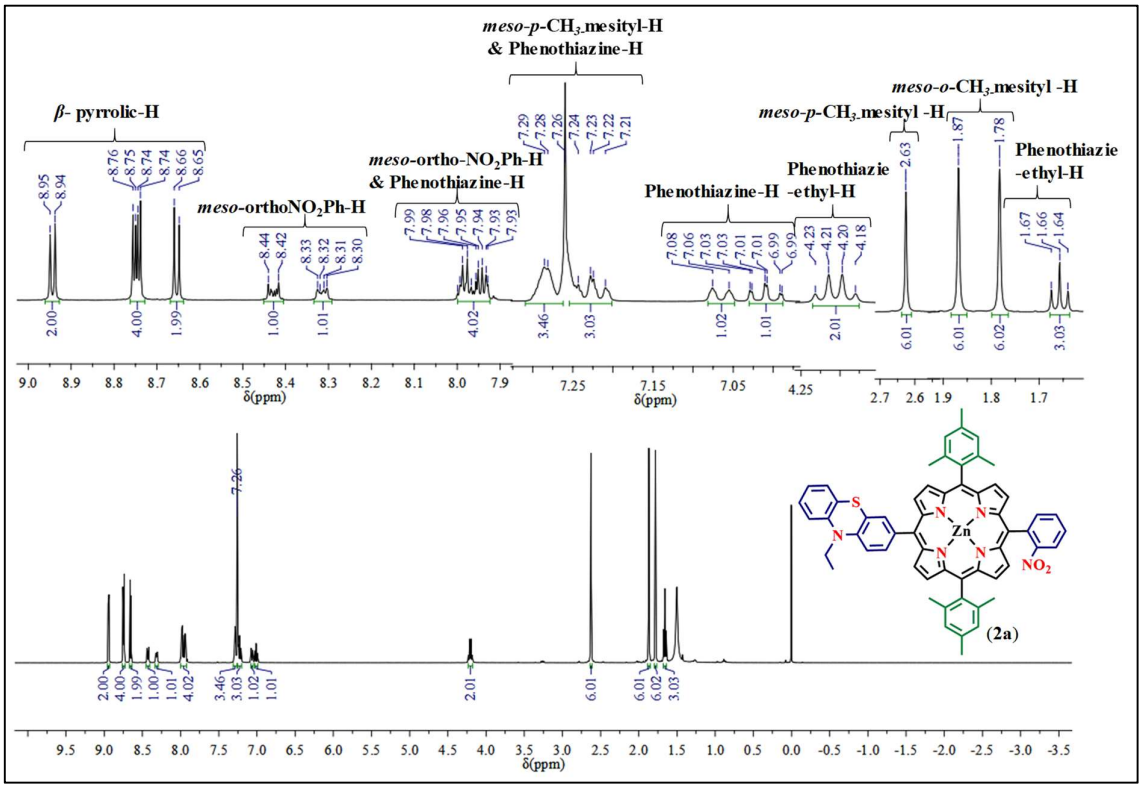

Figure S5 ^{1}H NMR of *trans*-ZnA$_2$BC (**2a**) in CDCl$_3$ at 298 K.

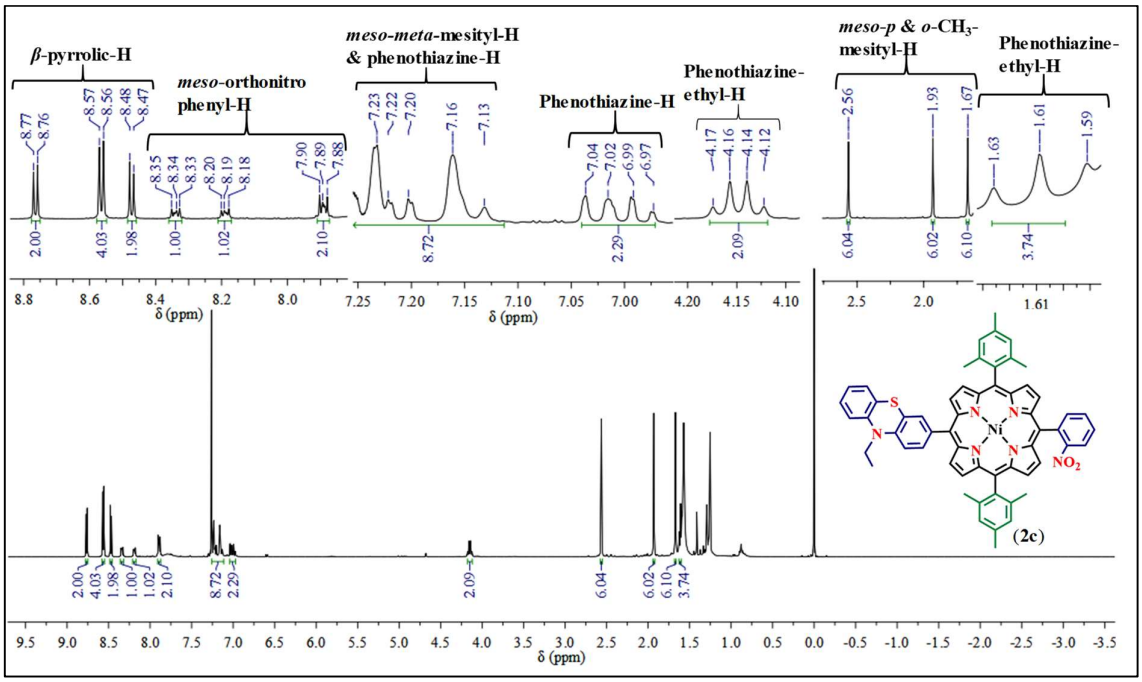

Figure S6 ^{1}H NMR of *trans*-NiA$_2$BC (**2c**) in CDCl$_3$ at 298 K.

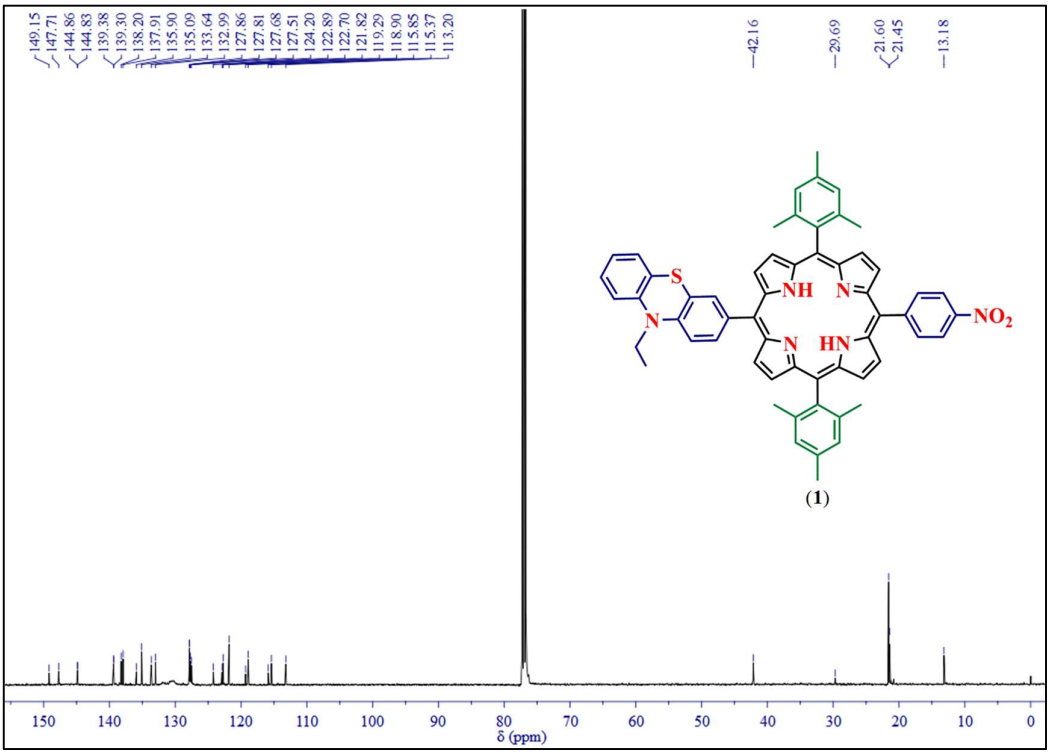

Figure S7 ^{13}C NMR of *trans*-H_2A_2BC (**1**) in $CDCl_3$ at 298 K.

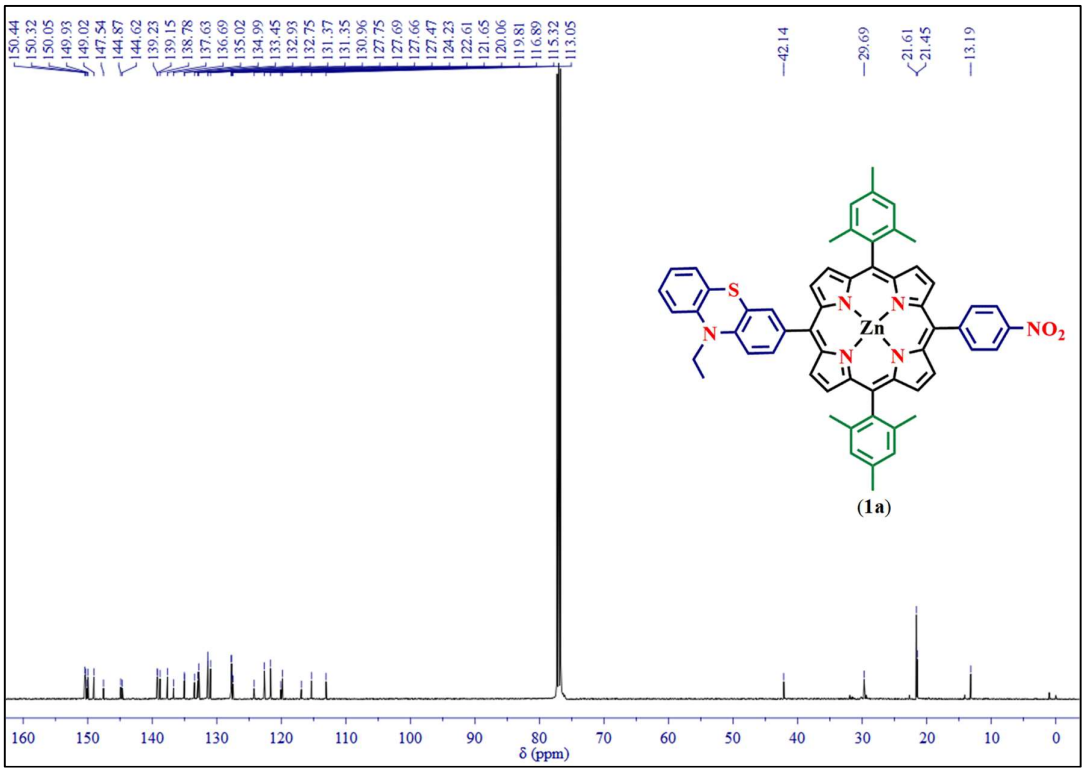

Figure S8 ^{13}C NMR of *trans*-ZnA_2BC (**1a**) in $CDCl_3$ at 298 K.

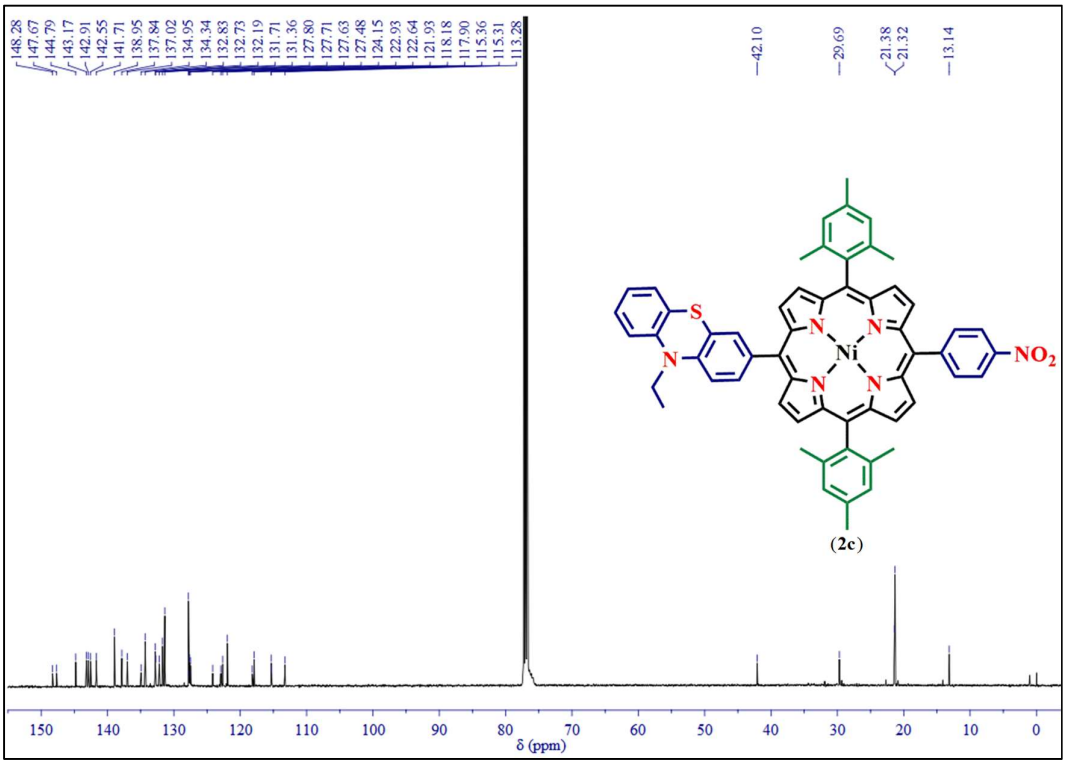

Figure S9 ^{13}C NMR of *trans*-NiA$_2$BC (**1c**) in CDCl$_3$ at 298 K.

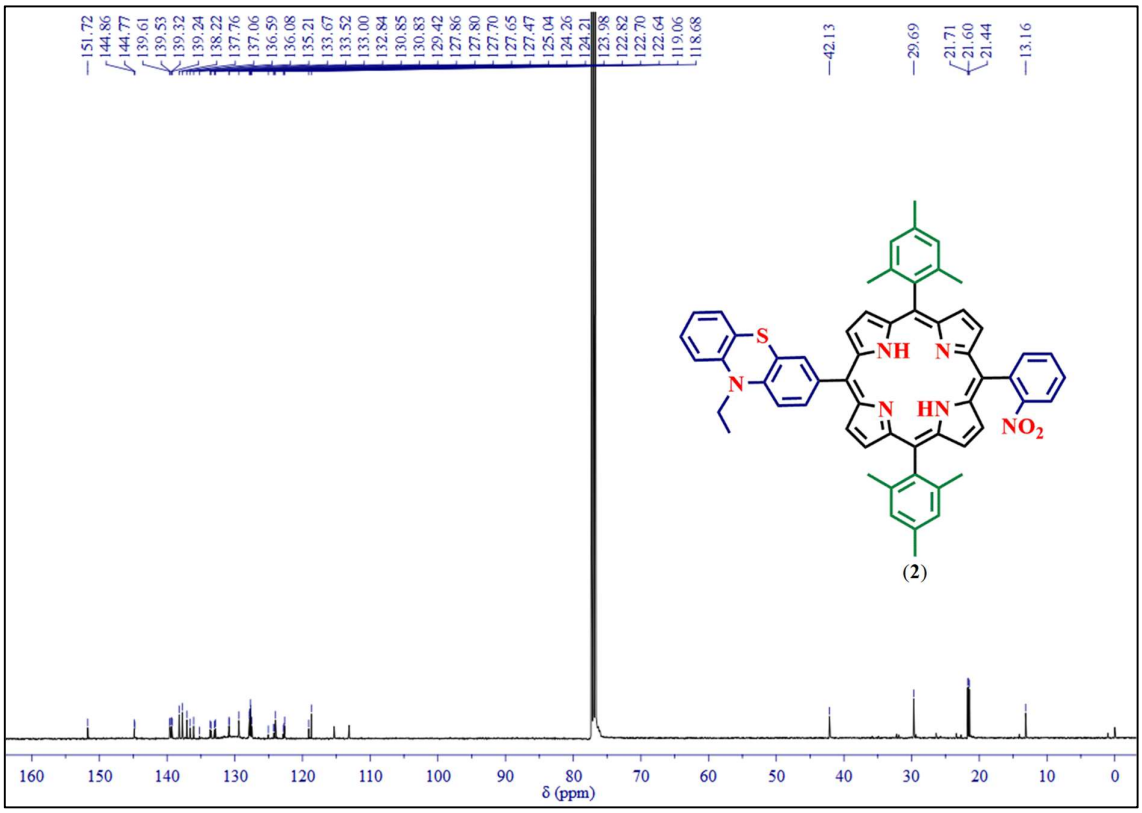

Figure S10 ^{13}C NMR of *trans*-H$_2$A$_2$BC (**2**) in CDCl$_3$ at 298 K.

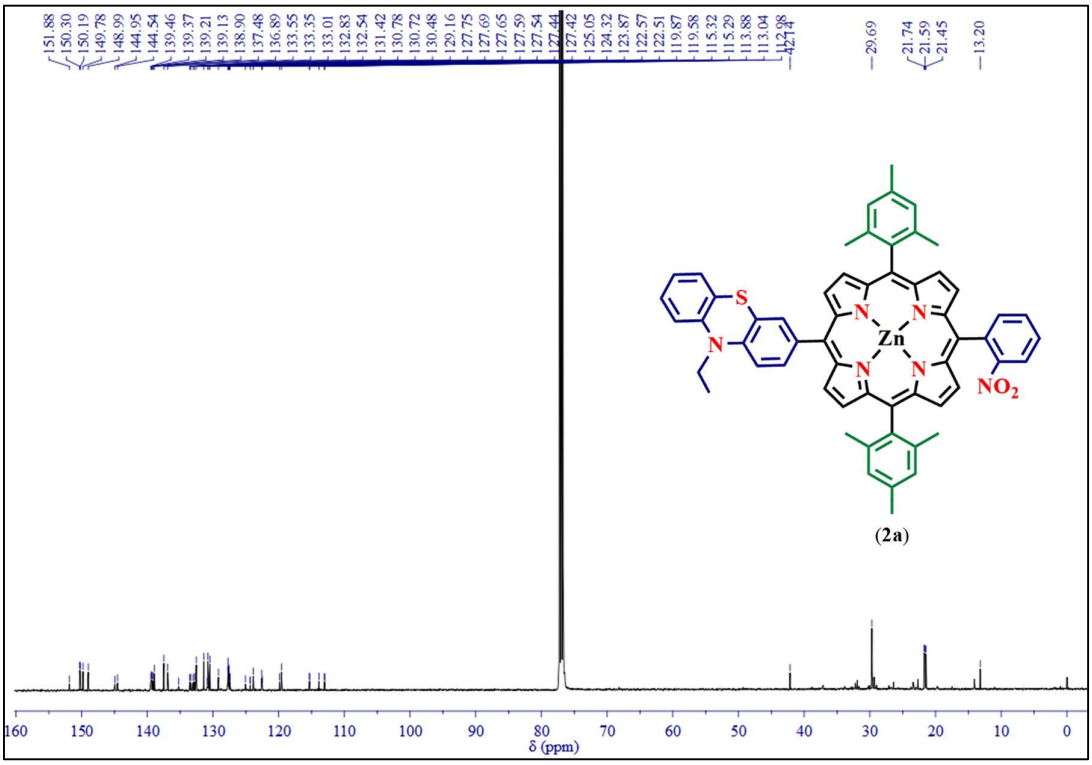

Figure S11 ^{13}C NMR of *trans*-ZnA_2BC (**2a**) in $CDCl_3$ at 298 K.

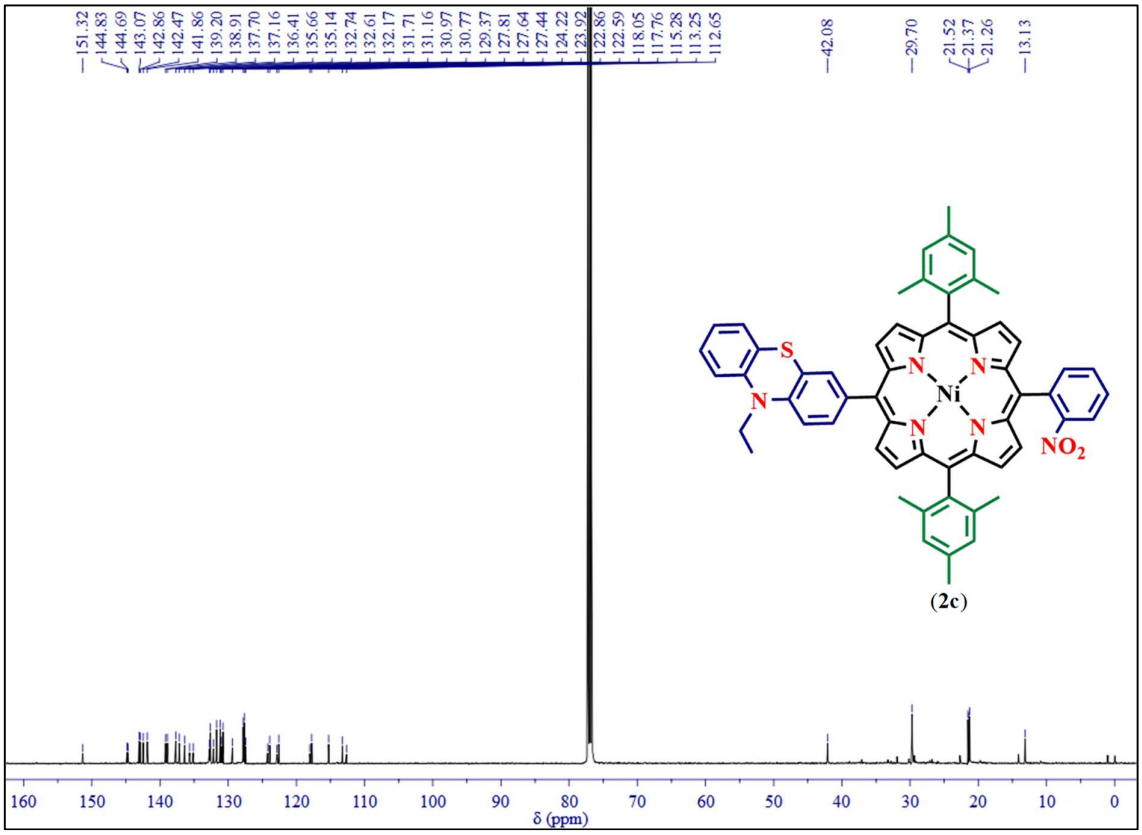

Figure S12 ^{13}C NMR of *trans*-NiA_2BC (**2c**) in $CDCl_3$ at 298 K.

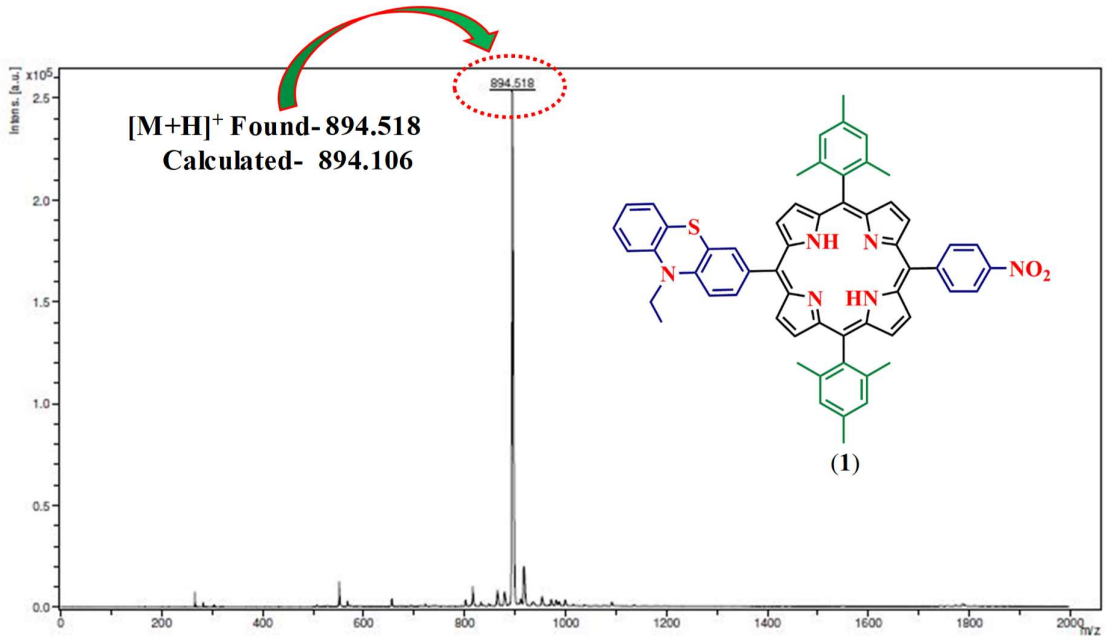

Figure S13 MALDI-TOF mass spectrum of *trans*-H_2A_2BC (**1**) in DCM in a positive ion mode.

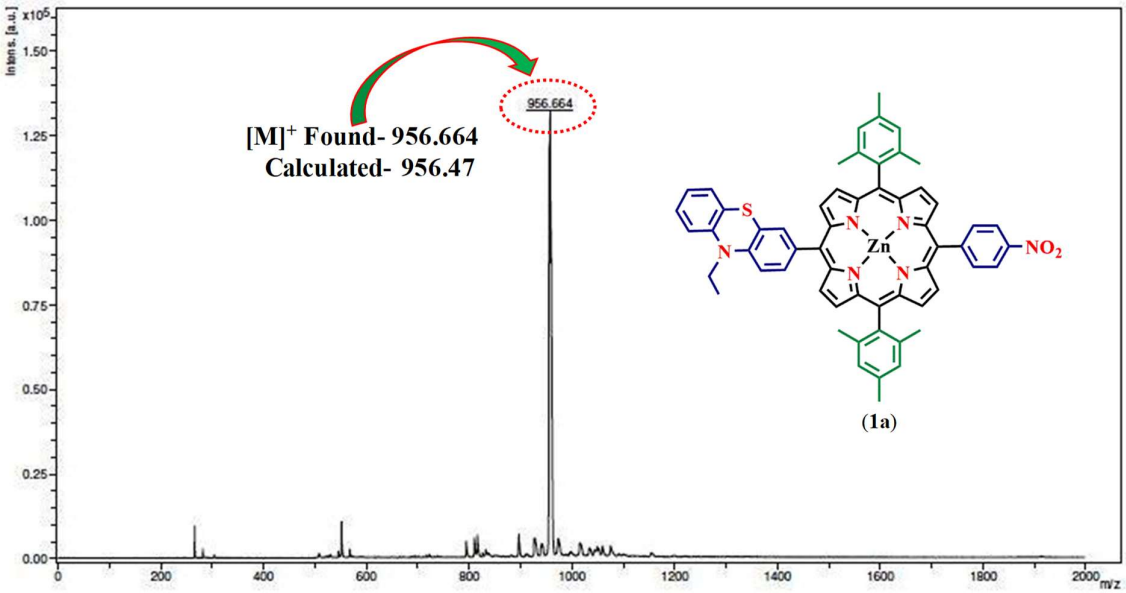

Figure S14 MALDI-TOF mass spectrum of *trans*-ZnA_2BC (**1a**) in DCM in a positive ion mode.

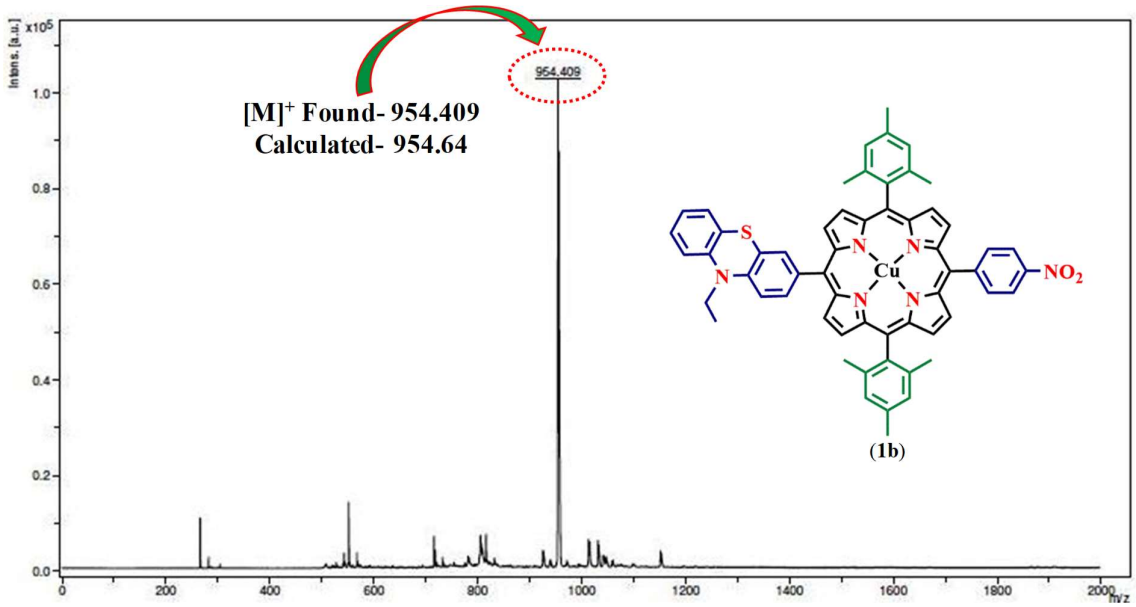

Figure S15 MALDI-TOF mass spectrum of *trans*-CuA_2BC (**1b**) in DCM in a positive ion mode.

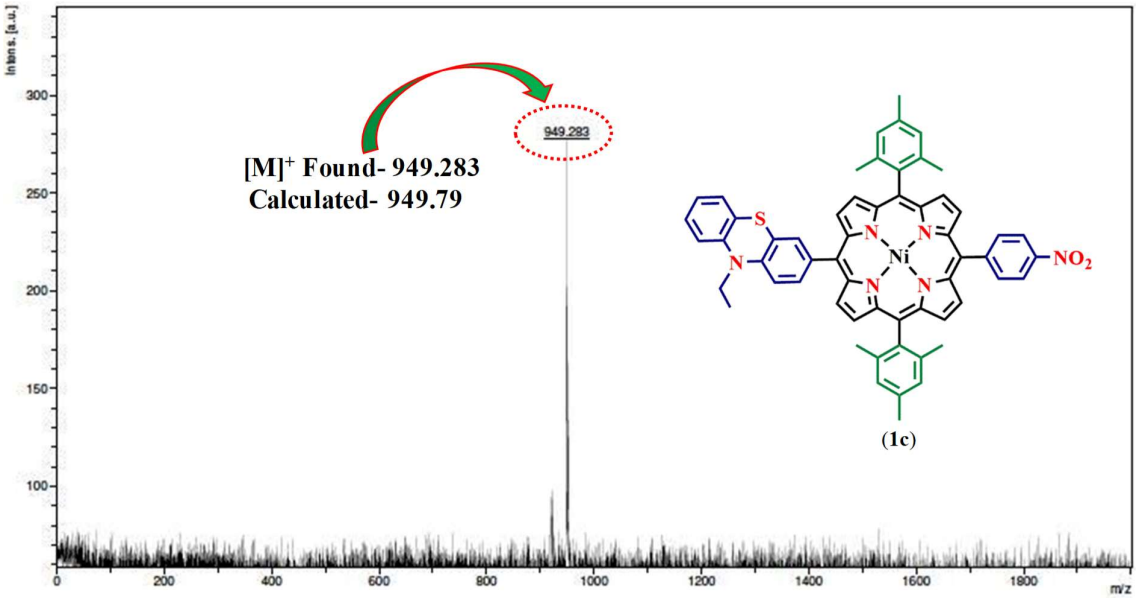

Figure S16 MALDI-TOF mass spectrum of *trans*-NiA_2BC (**1c**) in DCM in a positive ion mode.

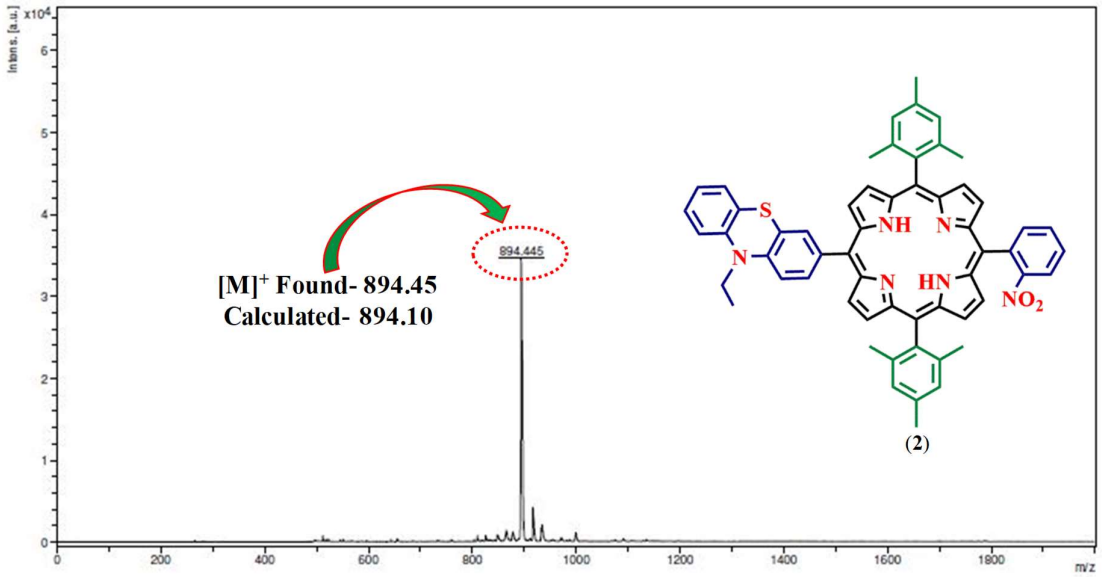

Figure S17 MALDI-TOF mass spectrum of *trans*-H_2A_2BC (**2**) in DCM in a positive ion mode.

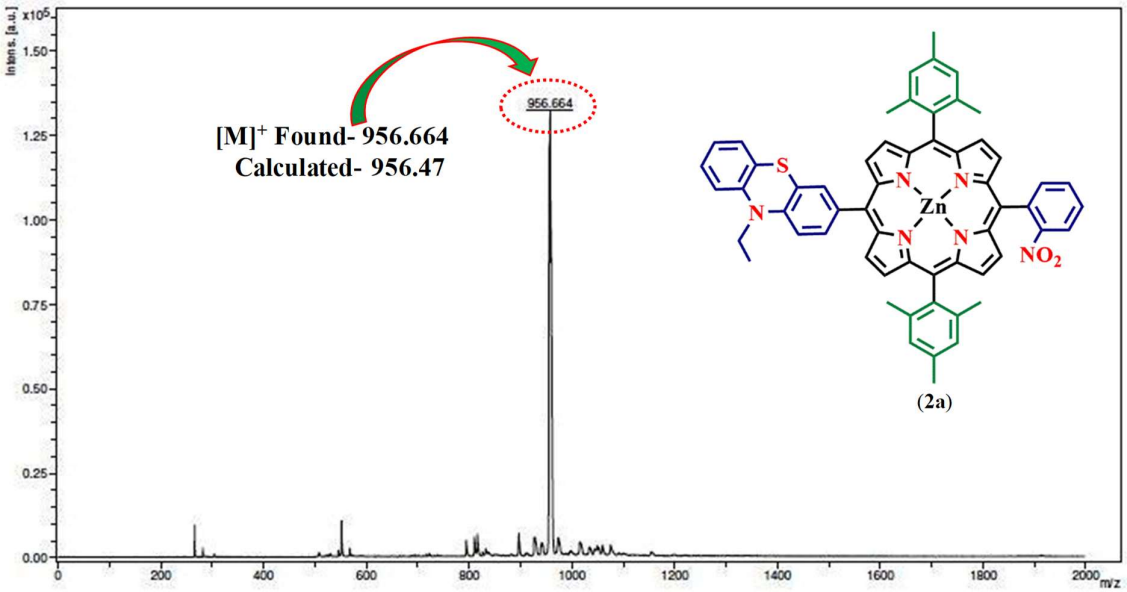

Figure S18 MALDI-TOF mass spectrum of *trans*-ZnA_2BC (**2a**) in DCM in a positive ion mode.

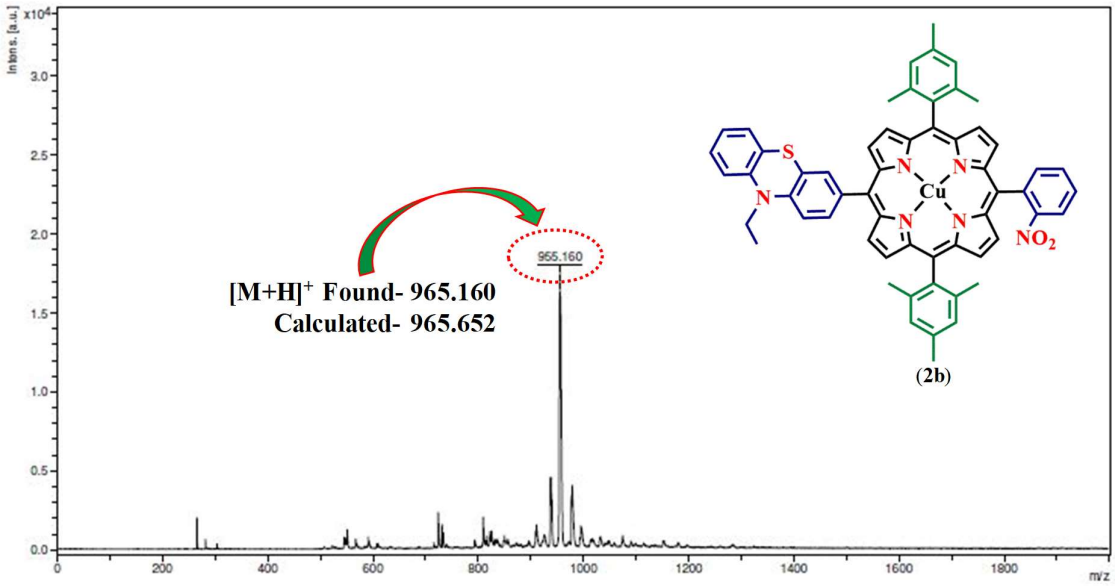

Figure S19 MALDI-TOF mass spectrum of *trans*-CuA_2BC (**2b**) in DCM in a positive ion mode.

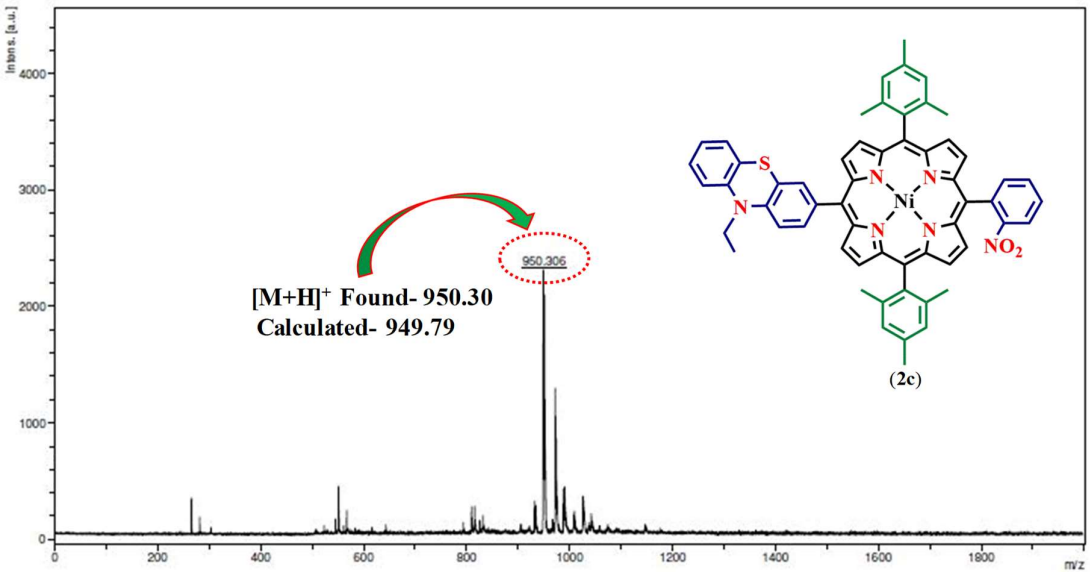

Figure S20 MALDI-TOF mass spectrum of *trans*-NiA_2BC (**2c**) in DCM in a positive ion mode.

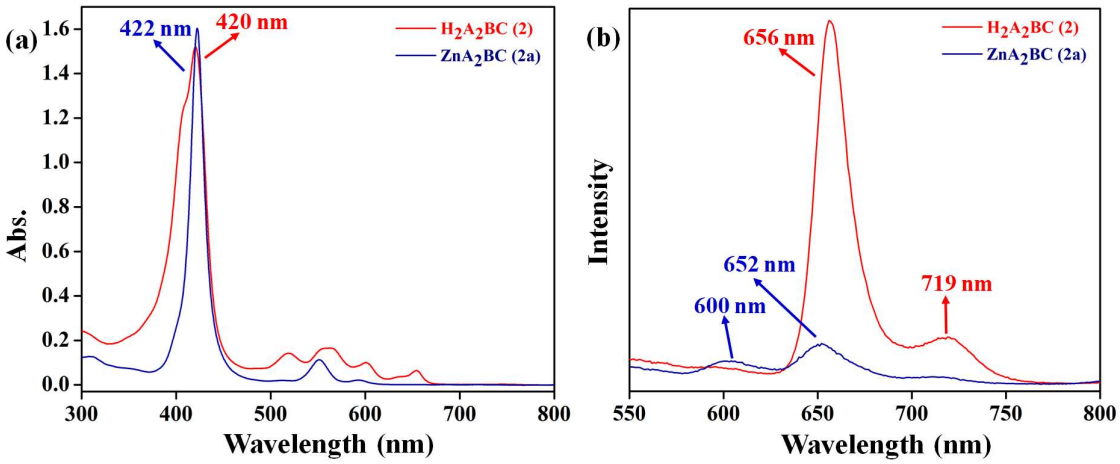

Figure S21 (a) UV-visible Spectra of *trans*-H_2A_2BC (**2**) and *trans*-ZnA_2BC (**2a**) in DCM at 298 K. (b) Emission Spectra of *trans*-H_2A_2BC (**2**) and *trans*-ZnA_2BC (**2a**) in DCM at 298 K.

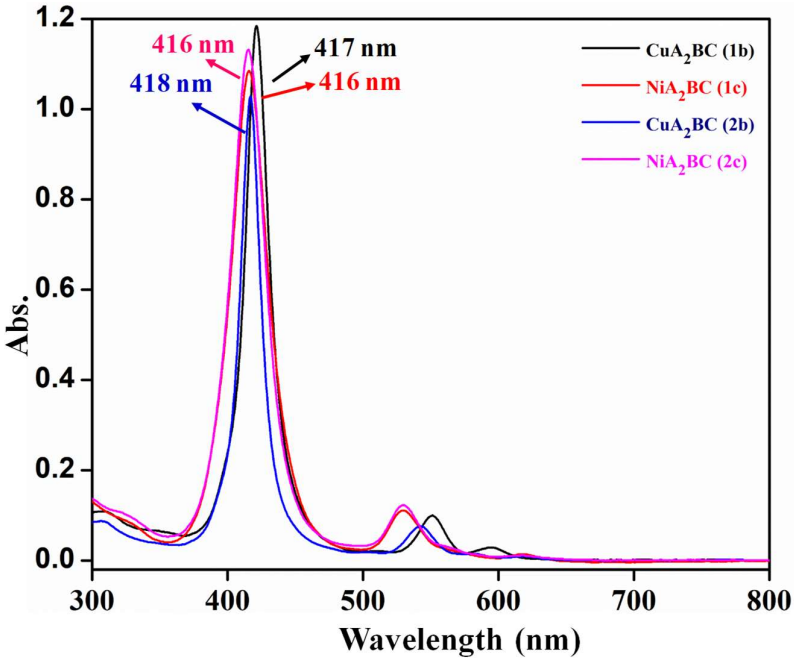

Figure S22 Comparative UV-visible spectra of *trans*-MA_2BC (M= Cu(II) (**1b**), Ni(II) (**1c**), Cu(II) (**2b**), and Ni(II) (**2c**))

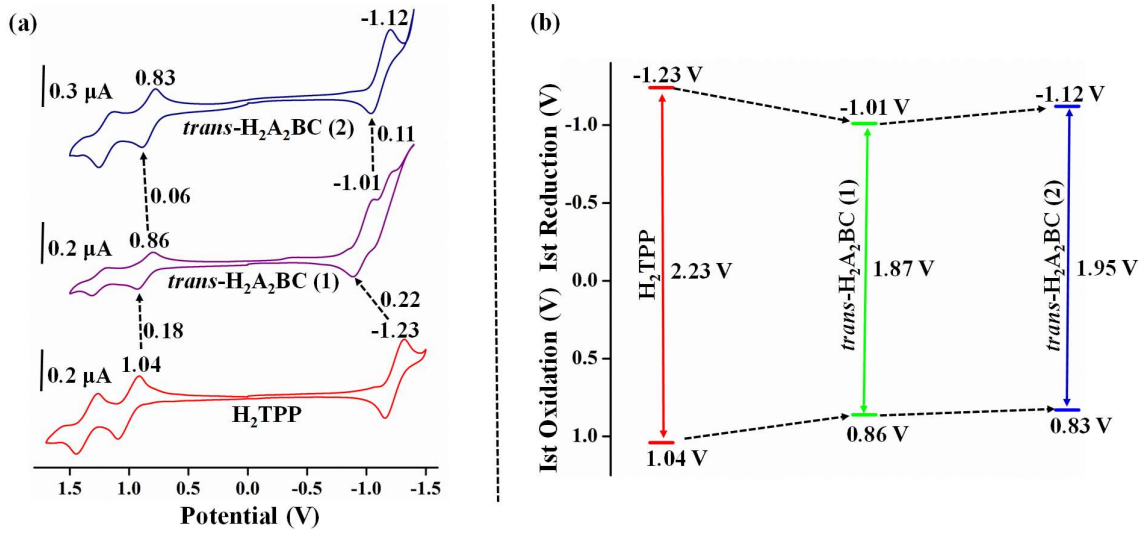

Figure S23 (**a**) Comparative cyclic voltammograms of *trans*-H_2A_2BC porphyrins **1** and **2** with respect to H_2TPP in CH_2Cl_2 containing $TBAPF_6$ as a supporting electrode at 298 K. (**b**) Energy level diagram of *trans*-H_2A_2BC porphyrins **1** and **2** with respect to H_2TPP.

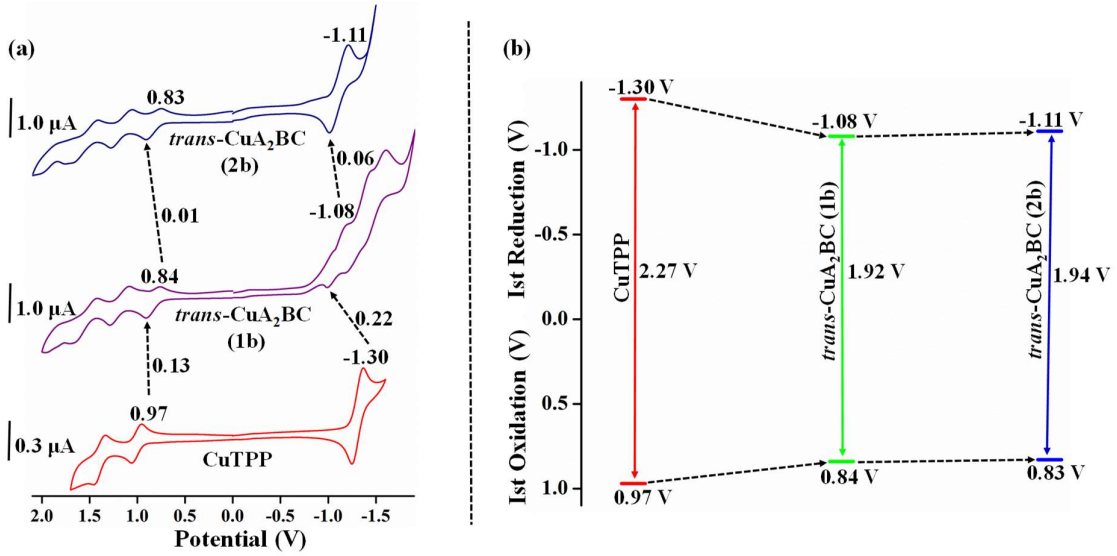

Figure S24 (**a**) Comparative cyclic voltammograms of *trans*-CuA_2BC porphyrins **1b** and **2b** with respect to CuTPP in CH_2Cl_2 containing $TBAPF_6$ as a supporting electrode at 298 K. (**b**) Energy level diagram of *trans*-CuA_2BC porphyrins **1b** and **2b** with respect to CuTPP.

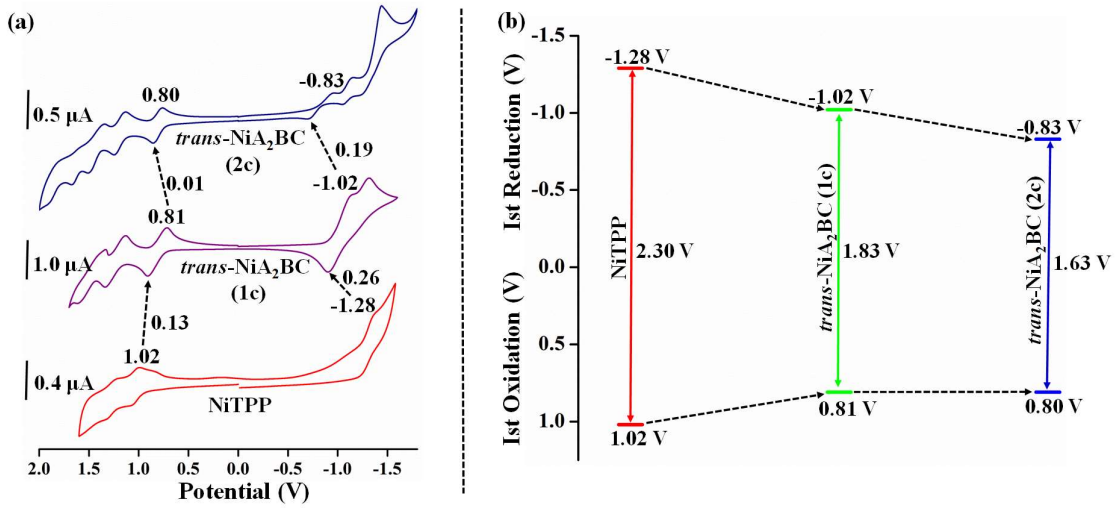

Figure S25 (**a**) Comparative cyclic voltammograms of *trans*-NiA_2BC porphyrins **1b** and **2b** with respect to NiTPP in CH_2Cl_2 containing $TBAPF_6$ as a supporting electrode at 298 K. (**b**) Energy level diagram of *trans*-NiA_2BC porphyrins **1b** and **2b** with respect to NiTPP.

Table S1 Crystallographic and structure refinement data for synthesized *trans*-H_2A_2BC porphyrin (**2**).

Formula	$C_{58}H_{48}N_6O_2S$
Formula weight	893.08
Crystal system	Triclinic
Space group	P-1
a, Å	8.0272 (16)
b, Å	17.522 (4)
c, Å	22.872 (5)
α, degrees	69.48 (3)
β, degrees	83.85 (3)
γ, degrees	81.25 (3)
V, $Å^3$	2972.8 (12)
D_{calc}, mg/m^3	0.998
Z	2

Crystal size, mm	0.19, 0.14, 0.08
λ (Mo Kα) Å	0.71073 Å
temperature, K	298 (2)
Data collection range, θ, deg.	1.890 to 25.252
Total reflections collected	63723
Independent reflections	10408
Quality-of-fit indicator	1.533
Final R indices [1> 2σ (I)]	R1 = 0.1395; wR2 = 0.3656
R indices (all data)	R1 = 0.1632; wR2 = 0.3857
CCDC No.	2050444

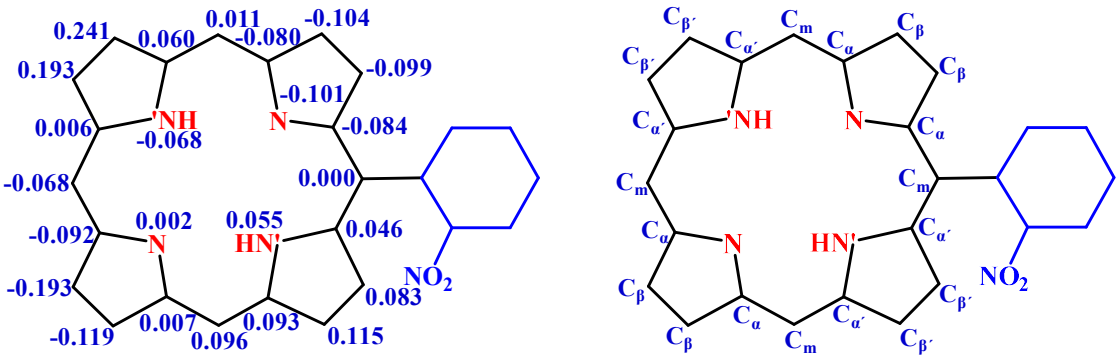

Figure S26 Deviation of core atoms of porphyrin ring from the mean plane for synthesized *trans*-H_2A_2BC porphyrin (**2**) from single crystal XRD structure.

Table S2 Selected average bond lengths and bond angles of synthesized *trans*-H_2A_2BC porphyrin (**2**) from single crystal XRD studies.

Bond Lengths (Å)		**Bond Angles (º)**	
N - Cα	1.370(2)	**N-Cα-Cβ**	108.8(2)
N′ - Cα′	1.365(7)	**N′- Cα′- Cβ′**	108.6(4)
Cα - Cβ	1.428(5)	**Cβ - Cα - Cm**	124.1(9)
Cα′ - Cβ′	1.445(7)	**Cβ′- Cα′ - Cm**	125.2(2)

C_β - C_β	1.362(5)	**C_α - C_m - C_α'**	124.7(7)
C_β' - C_β'	1.360	**C_α - C_β - C_β**	107.1(7)
C_α - C_m	1.394	**C_α'- C_β' - C_β'**	107.3(1)
C_α' - C_m	1.408	**C_α'- N′- C_α'**	108.0(6)
ΔC_β (Å)	0.143	**C_α - N- C_α**	107.9(5)
ΔC_{24} (Å)	0.080		

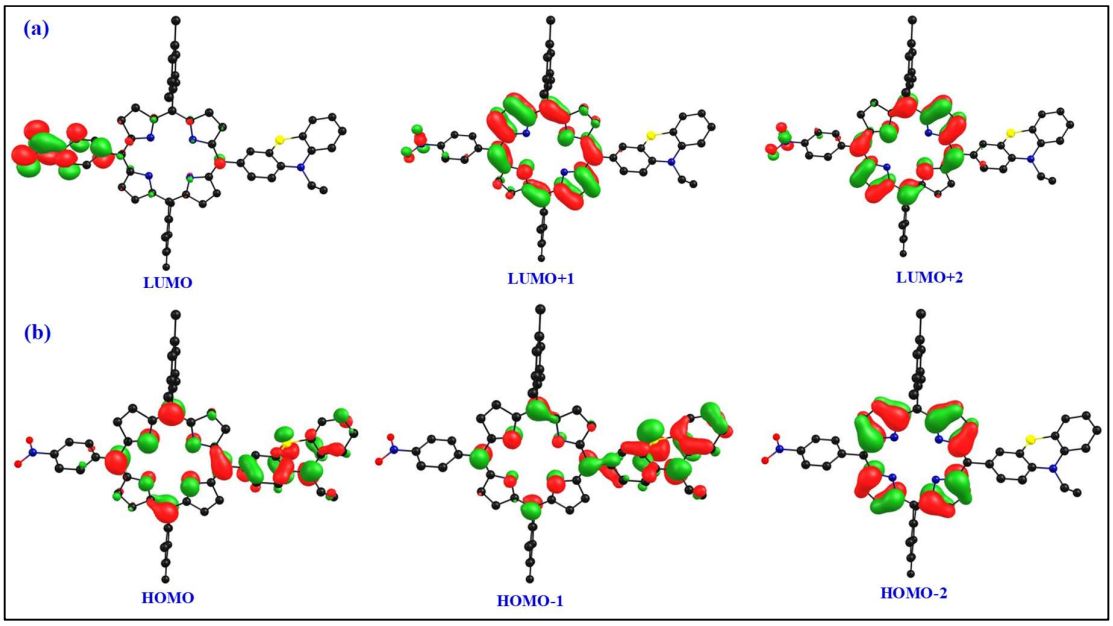

Figure S27 Frontier molecular orbitals of *trans*-H_2A_2BC (**1**) using DFT calculation at the B3LYZ/LANL2DZ level.

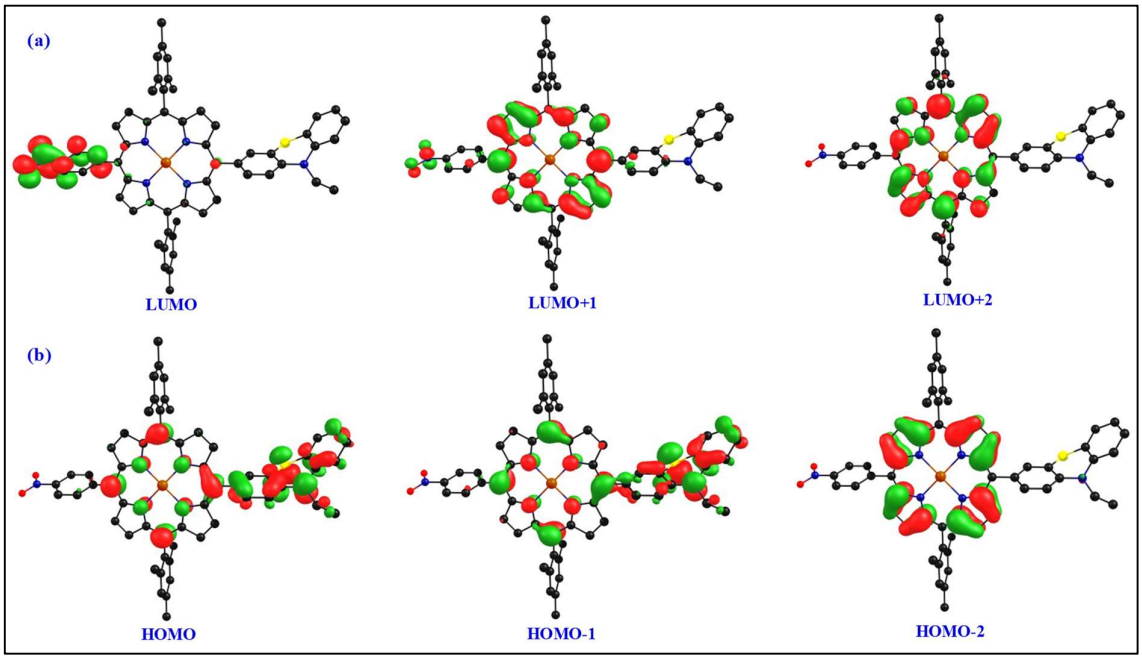

Figure S28 Frontier molecular orbitals of *trans*-ZnA_2BC (**1a**) using DFT calculation at the B3LYZ/LANL2DZ level.

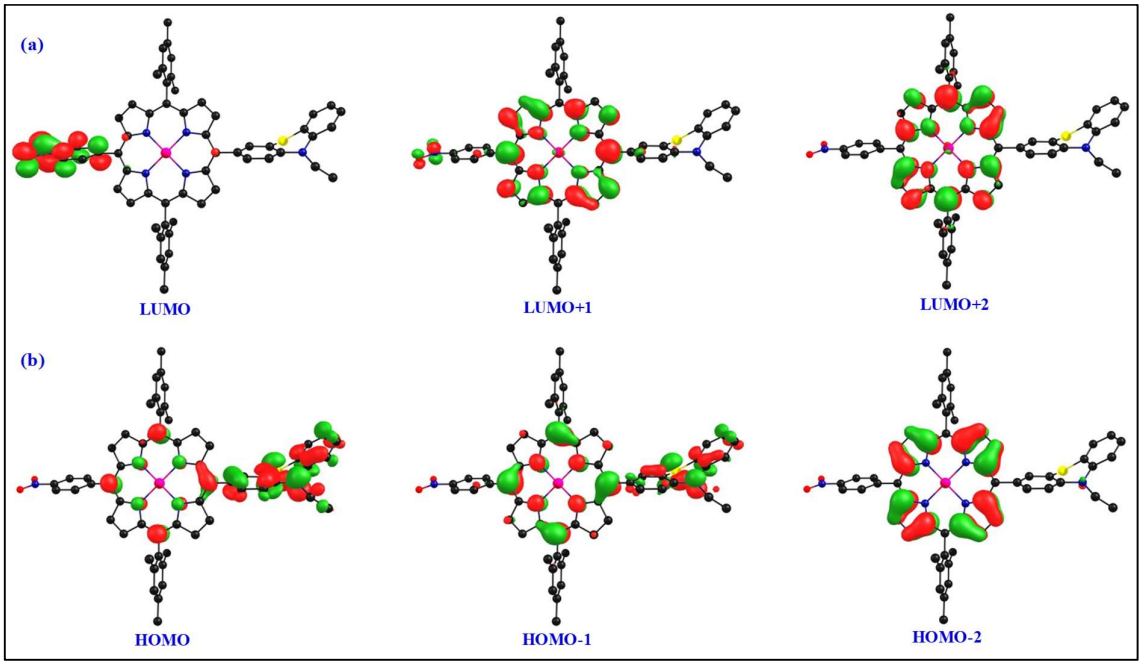

Figure S29 Frontier molecular orbitals of *trans*-CuA_2BC (**1b**) using DFT calculation at the B3LYZ/LANL2DZ level.

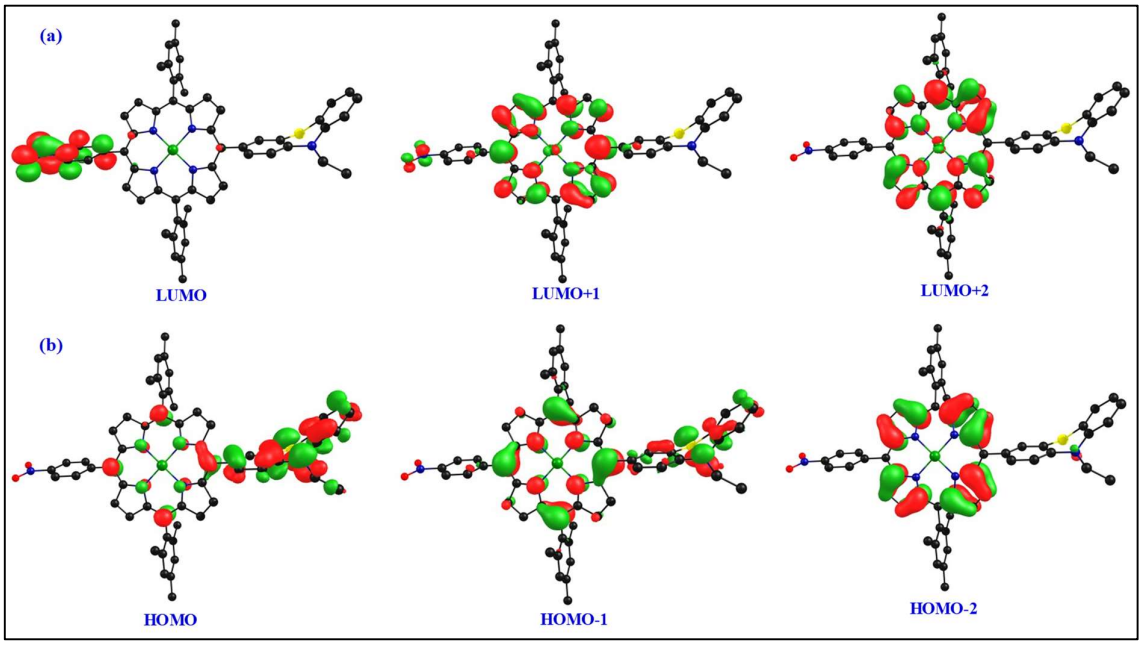

Figure S30 Frontier molecular orbitals of *trans*-NiA_2BC (**1c**) using DFT calculation at the B3LYZ/LANL2DZ level.

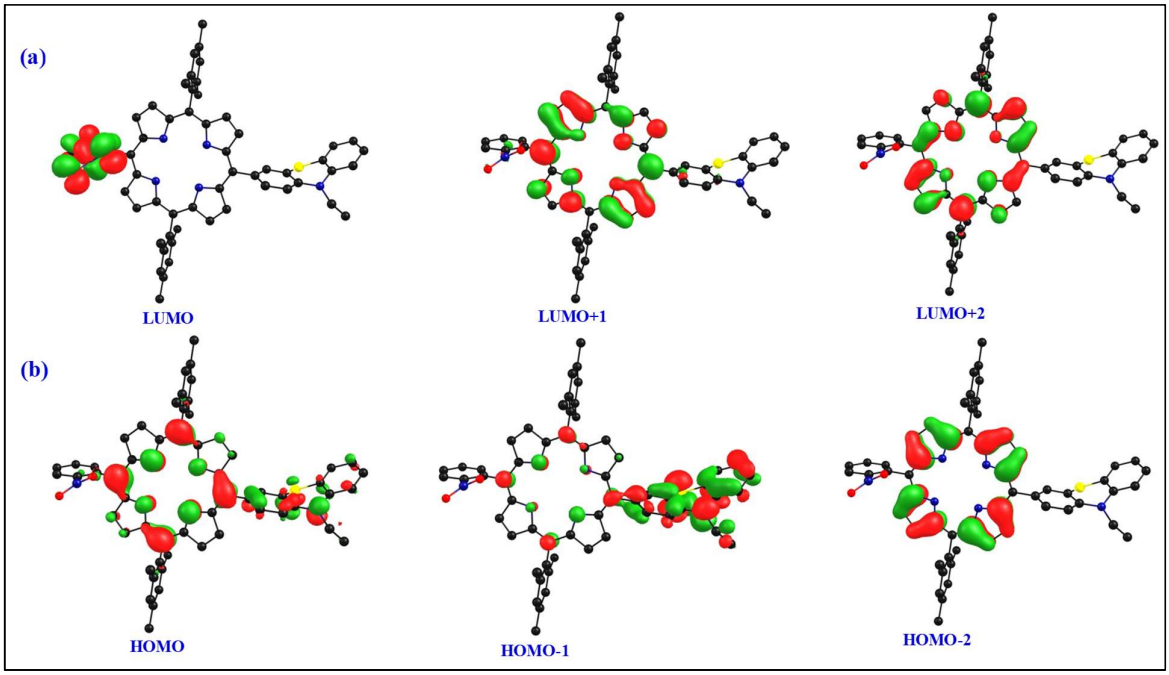

Figure S31 Frontier molecular orbitals of *trans*-H_2A_2BC (**2**) using DFT calculation at the B3LYZ/LANL2DZ level.

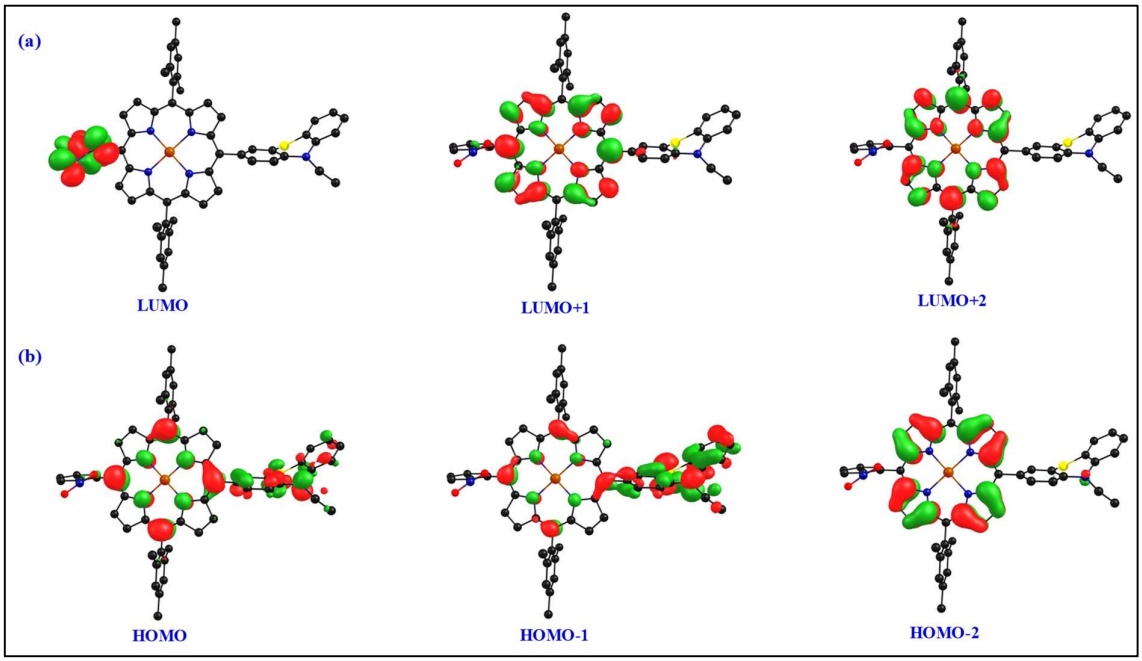

Figure S32 Frontier molecular orbitals of *trans*-ZnA_2BC (**2a**) using DFT calculation at the B3LYZ/LANL2DZ level.

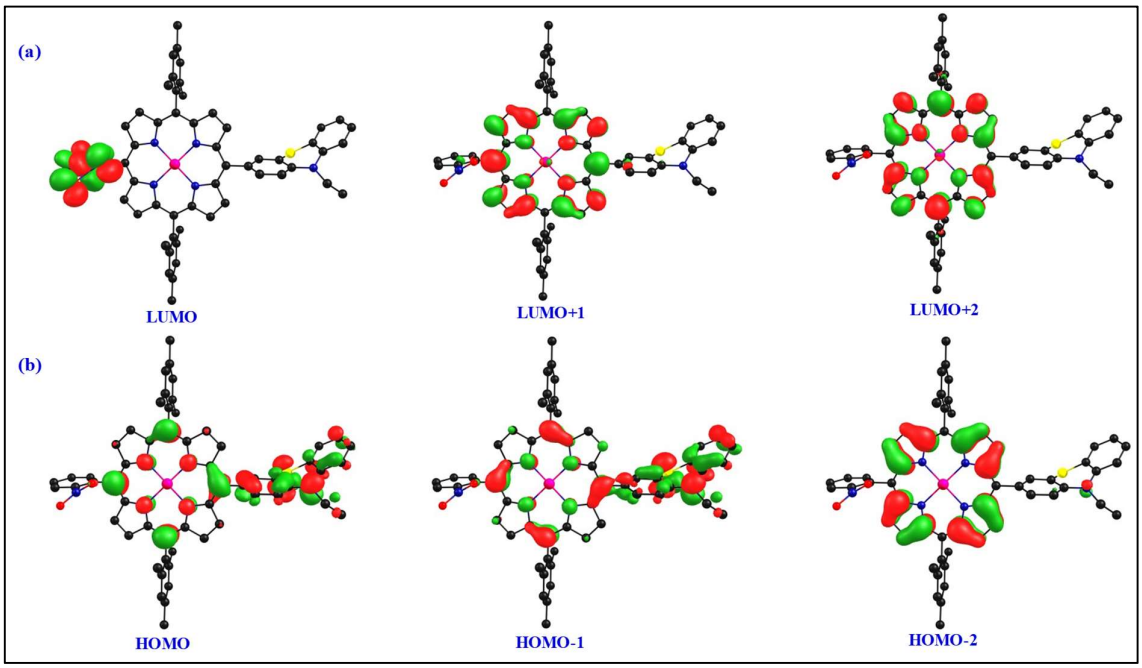

Figure S33 Frontier molecular orbitals of *trans*-CuA_2BC (**2b**) using DFT calculation at the B3LYZ/LANL2DZ level.

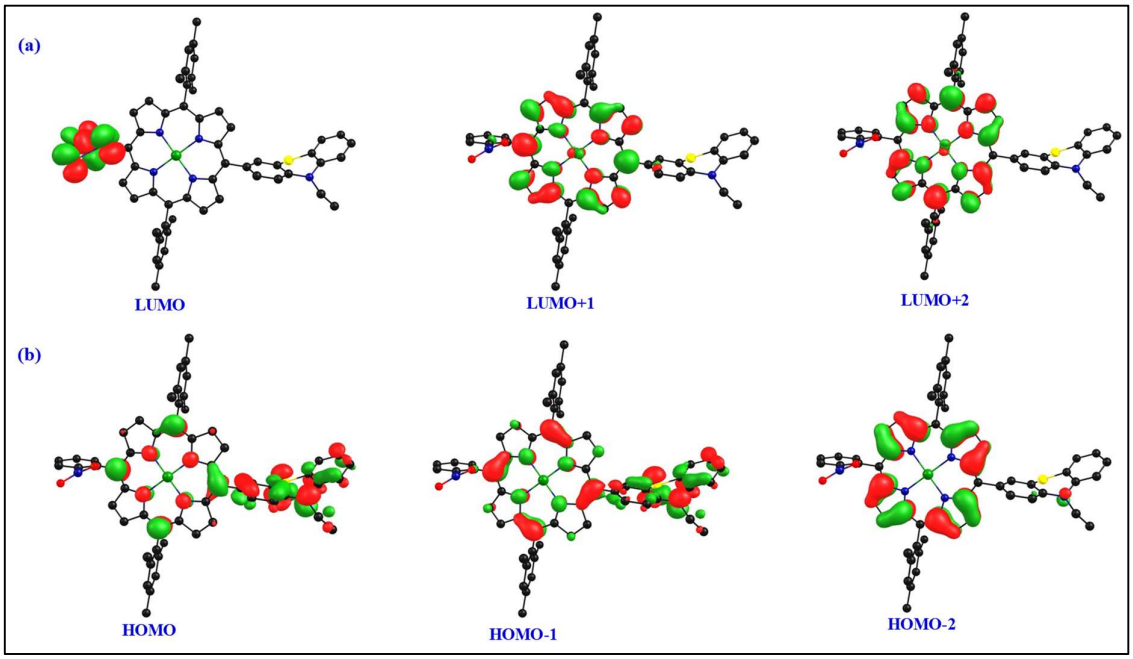

Figure S34 Frontier molecular orbitals of *trans*-NiA_2BC (**2c**) using DFT calculation at the B3LYZ/LANL2DZ level.

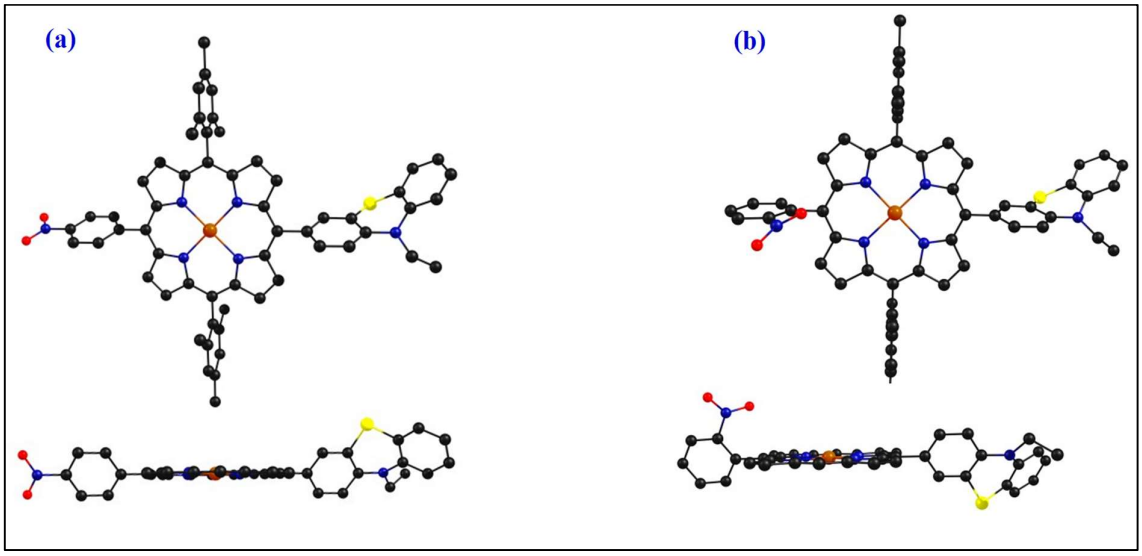

Figure S35 Optimized geometry structure for *trans*-ZnA_2BC **1a** and **2a**.

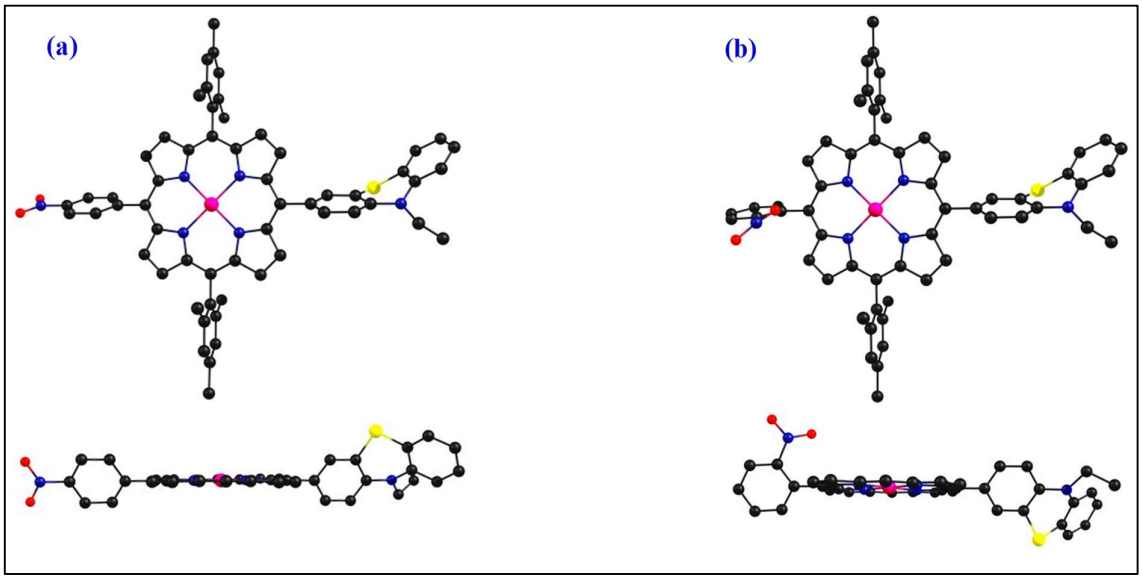

Figure S36 Optimized geometry structure for *trans*-CuA_2BC **1b** and **2b**.

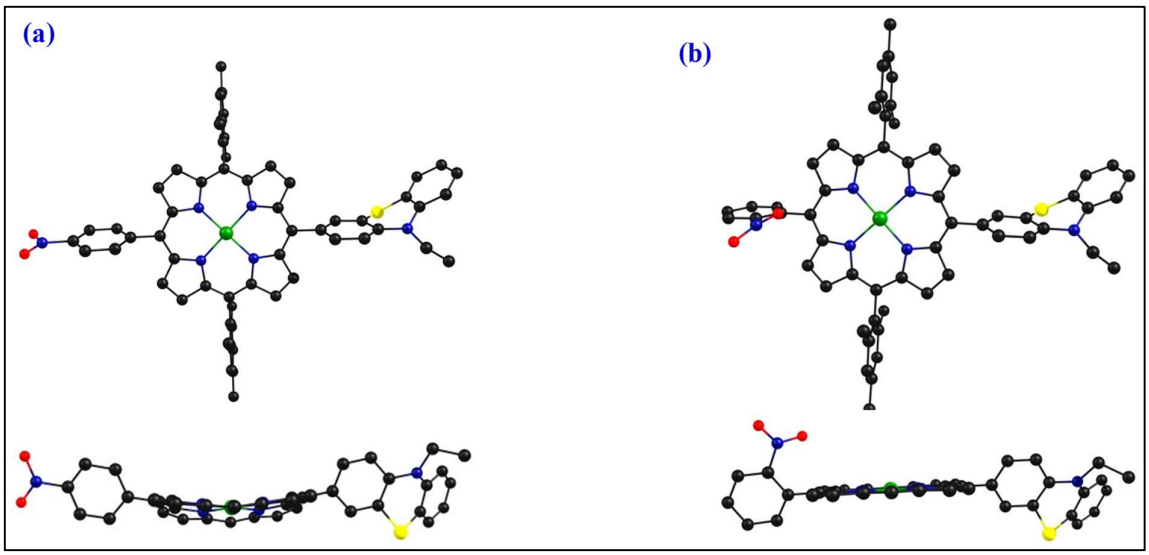

Figure S37 Optimized geometry structure for *trans*-NiA_2BC **1c** and **2c**.

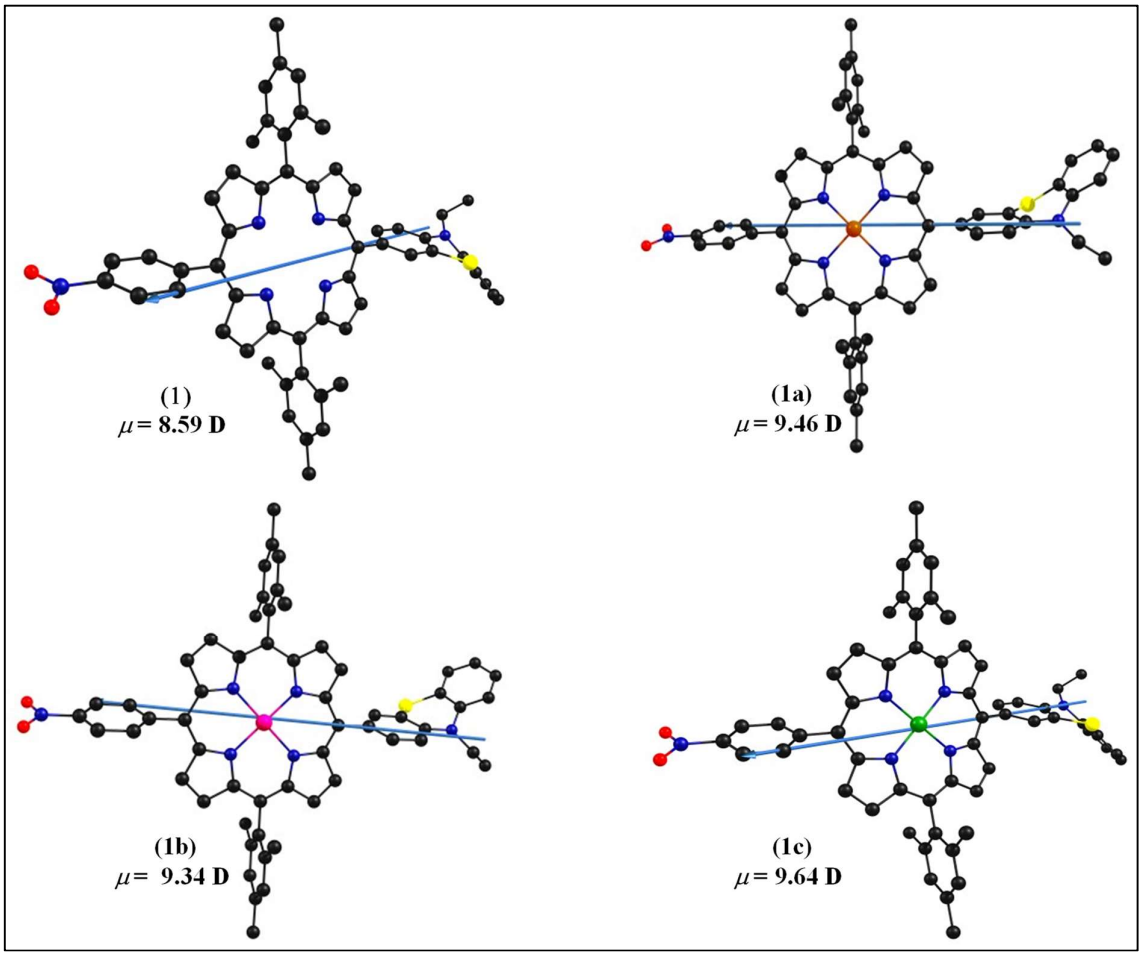

Figure S38 The pictorial representations of the resultant dipole moments of *trans*-A_2BC type porphyrins **1**, **1a**, **1b** and **1c**.

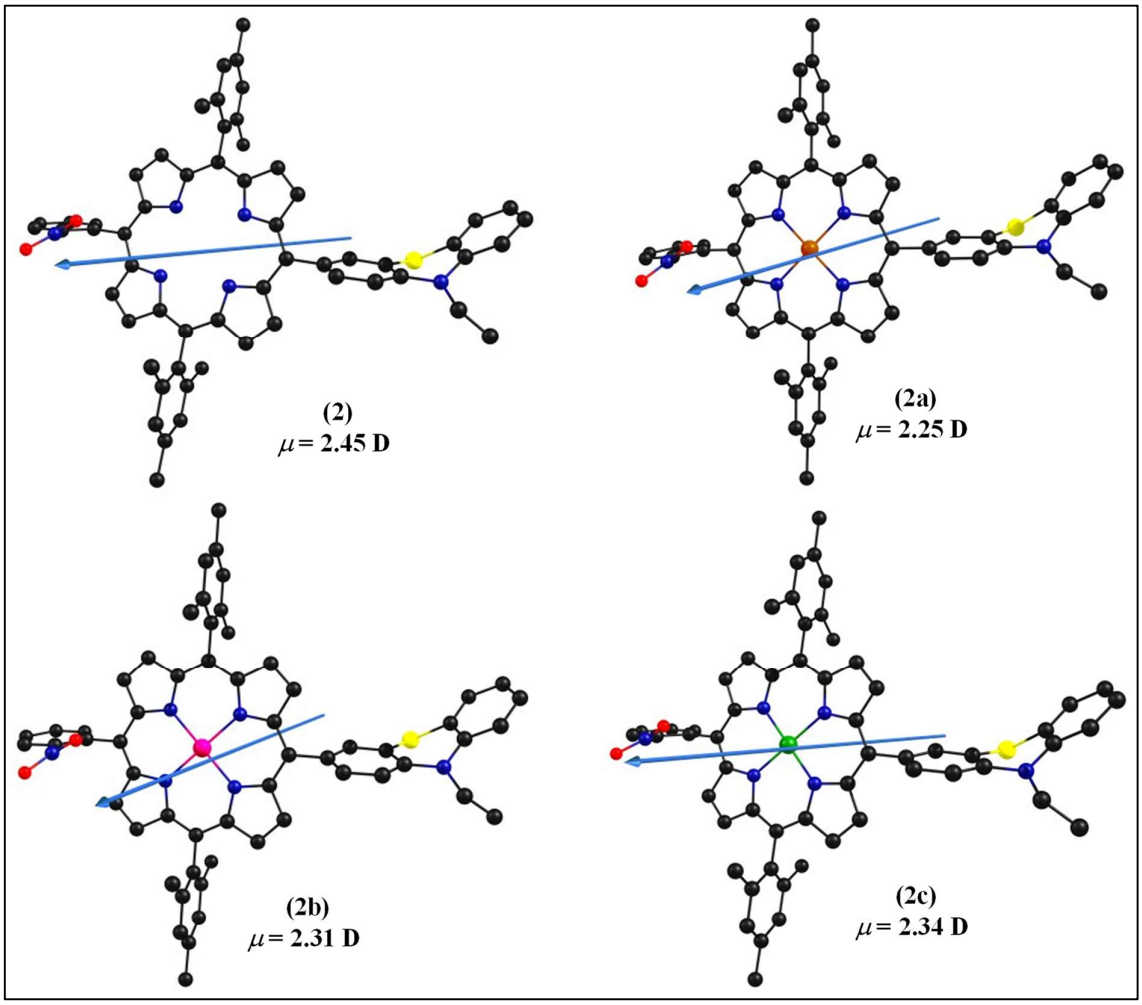

Figure S39 The pictorial representations of the resultant dipole moments of *trans*-A_2BC type porphyrins **2**, **2a**, **2b** and **2c**.

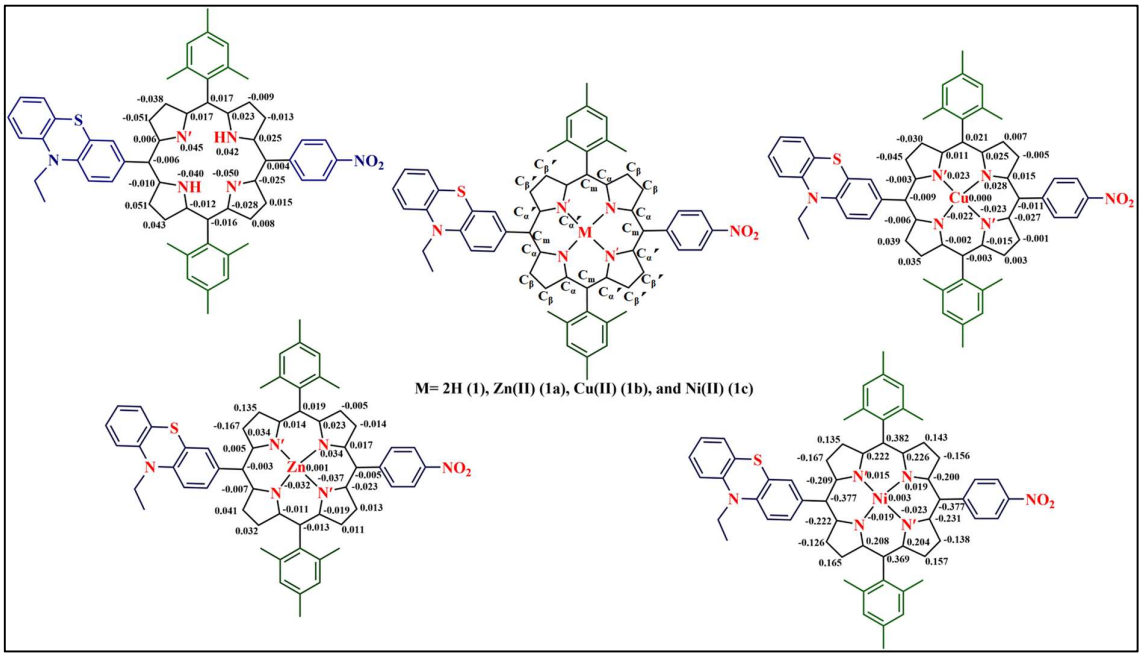

Figure S40 Deviation of core atoms of porphyrin ring from the mean plane for *trans*-A_2BC type porphyrins **1, 1a, 1b** and **1c**.

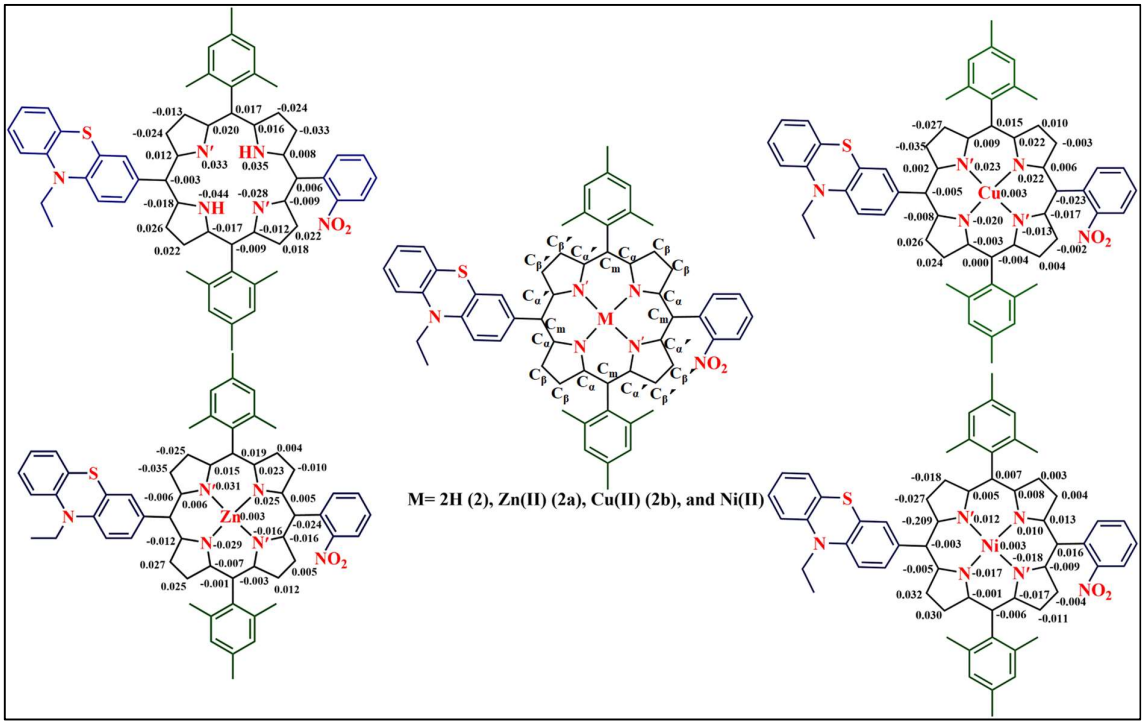

Figure S41 Deviation of core atoms of porphyrin ring from the mean plane for *trans*-A_2BC type porphyrins **2, 2a, 2b** and **2c**

Table S3 Selected bond lengths and bond angles of *trans*-A_2BC type porphyrins **1, 1a, 1b** and **1c**.

	1	1a	1b	1c
		Bond Length (A°)		
M-N	-	2.068	2.029	1.967
M-N′	-	2.068	2.029	1.967
N-C$_{\alpha}$	1.389	1.395	1.396	1.399
N′-C$_{\alpha}$′	1.391	1.395	1.397	1.399
C$_{\alpha}$-C$_{\beta}$	1.470	1.458	1.455	1.451
C$_{\alpha'}$-C$_{\beta'}$	1.446	1.458	1.455	1.451
C$_{\beta}$-C$_{\beta}$	1.368	1.375	1.372	1.370
C$_{\beta'}$-C$_{\beta'}$	1.382	1.375	1.372	1.370
C$_{\alpha}$-C$_{m}$	1.417	1.416	1.407	1.399
C$_{\alpha'}$-C$_{m}$	1.412	1.416	1.407	1.400
ΔC$_{\beta}$ (Å)	0.029	0.052	0.021	0.148
Δ24 (Å)	0.025	0.030	0.017	0.187
ΔMetal (Å)	-	0.001	0.000	0.003
		Bond Angles (°)		
M-N-C$_{\alpha}$	-	126.4	126.9	127.4
M-N′-C$_{\alpha}$	-	126.4	126.9	127.4
N-M-N	-	179.9	179.8	179.8
N′-M-N′	-	179.9	179.8	179.8
N-C$_{\alpha}$-C$_{m}$	126.4	126.1	126.4	126.2
N′-C$_{\alpha'}$-C$_{m}$	126.9	126.1	126.4	126.2
N-C$_{\alpha}$-C$_{\beta}$	110.4	109.1	109.7	110.3
N′-C$_{\alpha'}$-C$_{\beta'}$	106.6	109.1	109.7	110.3
C$_{\beta}$- C$_{\alpha}$-C$_{m}$	123.2	124.7	123.9	123.3
C$_{\beta'}$- C$_{\alpha'}$-C$_{m}$	126.6	124.7	123.9	123.4
C$_{\alpha}$-C$_{m}$-C$_{\alpha'}$	124.9	124.8	123.3	121.4
C$_{\alpha}$-C$_{\beta}$-C$_{\beta}$	106.7	107.3	107.2	107.1
C$_{\alpha'}$-C$_{\beta'}$-C$_{\beta'}$	108.2	107.3	107.2	107.1
C$_{\alpha'}$-N′-C$_{\alpha'}$	110.4	107.1	106.2	105.2
C$_{\alpha}$-N-C$_{\alpha}$	105.7	107.1	106.2	105.2

Table S4 Selected bond lengths and bond angles of *trans*-A$_2$BC type porphyrins **2, 2a, 2b** and **2c**.

	2	2a	2b	2c
		Bond Length (A°)		
M-N	-	2.067	2.028	1.982
M-N′	-	2.067	2.028	1.982
N-C$_{\alpha}$	1.390	1.394	1.396	1.399

N′-C$_{\alpha}$′	1.389	1.394	1.396	1.400
C$_{\alpha}$-C$_{\beta}$	1.446	1.458	1.455	1.451
C$_{\alpha'}$-C$_{\beta'}$	1.470	1.458	1.455	1.450
C$_{\beta}$-C$_{\beta}$	1.382	1.375	1.372	1.369
C$_{\beta'}$-C$_{\beta'}$	1.368	1.375	1.372	1.369
C$_{\alpha}$-C$_{m}$	1.410	1.414	1.405	1.397
C$_{\alpha'}$-C$_{m}$	1.415	1.414	1.406	1.397
ΔC$_{\beta}$ (Å)	0.023	0.018	0.016	0.016
Δ24 (Å)	0.019	0.016	0.013	0.019
ΔMetal (Å)	-	0.003	0.003	0.003
		Bond Angles (º)		
M-N-C$_{\alpha}$	-	126.5	126.9	127.6
M-N′-C$_{\alpha}$	-	126.4	126.9	127.6
N-M-N	-	179.3	179.8	179.9
N′-M-N′	-	178.8	179.5	180.0
N-C$_{\alpha}$-C$_{m}$	126.8	126.1	126.4	126.5
N′-C$_{\alpha'}$-C$_{m}$	126.3	126.0	126.4	126.5
N-C$_{\alpha}$-C$_{\beta}$	106.6	109.1	109.7	110.6
N′-C$_{\alpha'}$-C$_{\beta'}$	110.5	109.1	109.7	110.6
C$_{\beta}$- C$_{\alpha}$-C$_{m}$	123.2	124.8	123.9	122.9
C$_{\beta'}$- C$_{\alpha'}$-C$_{m}$	126.6	124.8	123.9	121.9
C$_{\alpha}$-C$_{m}$-C$_{\alpha'}$	124.97	124.9	123.5	121.9
C$_{\alpha}$-C$_{\beta}$-C$_{\beta}$	108.2	107.3	107.2	107.0
C$_{\alpha'}$-C$_{\beta'}$-C$_{\beta'}$	106.7	107.3	107.2	107.0
C$_{\alpha'}$-N′-C$_{\alpha'}$	110.4	107.1	106.2	104.8
C$_{\alpha}$-N-C$_{\alpha}$	105.6	126.5	106.2	104.8